7414 J. Med. Chem. 2010, 53, 7414–7427
DOI: 10.1021/jm100884b

Journal of Medicinal Chemistry Article

Discovery of Novel 2-Aryl-4-benzoyl-imidazoles Targeting the Colchicines Binding Site in Tubulin As Potential Anticancer Agents

Jianjun Chen,[†] Zhao Wang,[†] Chien-Ming Li,[‡,§] Yan Lu,[†] Pavan K. Vaddady,[†] Bernd Meibohm,[†] James T. Dalton,[‡,§] Duane D. Miller,[†,§] and Wei Li*[,†]

[†]Department of Pharmaceutical Sciences, University of Tennessee Health Science Center, Memphis, Tennessee 38163, United States, [‡]Division of Pharmaceutics, College of Pharmacy, The Ohio State University, Columbus, Ohio 43210, United States, and [§]GTx, Inc., Memphis, Tennessee 38163, United States

Received July 14, 2010

A series of 2-aryl-4-benzoyl-imidazoles (ABI) was synthesized as a result of structural modifications based on the previous set of 2-aryl-imidazole-4-carboxylic amide (AICA) derivatives and 4-substituted methoxylbenzoyl-aryl-thiazoles (SMART). The average IC_{50} of the most active compound (**5da**) was 15.7 nM. ABI analogues have substantially improved aqueous solubility (48.9 μg/mL for **5ga** vs 0.909 μg/mL for **SMART-1**, 0.137 μg/mL for paclitaxel, and 1.04 μg/mL for combretastatin A4). Mechanism of action studies indicate that the anticancer activity of ABI analogues is through inhibition of tubulin polymerization by interacting with the colchicine binding site. Unlike paclitaxel and colchicine, the ABI compounds were equally potent against multidrug resistant cancer cells and the sensitive parental melanoma cancer cells. In vivo results indicated that **5cb** was more effective than DTIC in inhibiting melanoma xenograph tumor growth. Our results suggest that the novel ABI compounds may be developed to effectively treat drug-resistant tumors.

Introduction

Cancer is one of the main causes of death, ranked only after heart disease. While existing therapies are effective in treating various cancers in their early stages, efficacy against metastatic cancers is far from satisfactory. With the rapid increasing of cancers in the U.S. and worldwide, clearly, there is an urgent need to develop highly effective anticancer drugs, which is the goal of our research. We previously described 2-aryl-imidazole-4-carboxylic amide (AICA[a]) derivatives (Figure 1) as potent antiproliferative agents for melanoma.[1] The most potent compounds in the AICA series have average IC_{50} values ranging from 3.5 to 10 μM on melanoma cells.[1] More recently, we reported a series of novel substituted methoxylbenzoyl-aryl-thiazole (SMART) compounds that possess nanomolar activity in inhibiting melanoma and prostate cancer cell growth in vitro.[2] Preliminary studies showed that the SMART compounds disrupt tubulin polymerization and therefore effectively prevent the formation of functional microtubules and block cell mitosis.[2] SMART compounds also showed great promise in overcoming P-glycoprotein (Pgp) mediated MDR in vitro.[3] Despite the high activity, most SMART compounds are hydrophobic and have limited water solubility, which requires extensive use of surfactants to solubilize a sufficient amount of drug for effective dosing or the use of advanced drug delivery strategies.[3] In addition, it has been reported that the thiazole ring, which is present in the SMART compounds, may undergo oxidative cleavage, resulting in a nitroxide and ultimately in reduced in vivo stability for SMART compounds.[4]

We hypothesized that replacing the thiazole ring of the SMART compounds with an imidazole to give aryl-benzoyl-imidazoles (ABI) would be highly beneficial for the following reasons. First, the imidazole moiety is present in many existing drugs and has been proven to be very stable.[5] Second, compared with the thiazole ring, the imidazole ring is much more hydrophilic, is expected to have improved aqueous solubility, and thus may simplify formulation and in vivo use. Finally, the imidazole is slightly acidic under physiological conditions. It is well-known that the microenvironment inside a tumor is slightly acidic because of a higher production of lactic acid from glycolysis (the Warburg effect).[6] The ABI analogues should exist predominantly in the un-ionized state under these conditions. As a result, ABI analogues may more easily pass through the cancer cell membrane and conceivably achieve higher intratumoral drug concentrations and greater in vivo potency.

In this paper, we describe our efforts to synthesize a focused set of ABI analogues (Figure 1) to understand their structure–activity relationships, to assess their efficacy in vivo, and to further elucidate their mechanism of action. The ABI analogues consist of three conjugated aromatic rings (denoted as rings A, B, and C in Figure 1). An imidazole ring was introduced as the B ring in the ABI series to replace the thiazole ring in the SMART series. The linker between the B and C rings was

*To whom correspondence should be addressed. Phone: (901)448-7532. Fax: (901)448-6828. E-mail: wli@uthsc.edu.

[a]Abbreviations: ABI, 2-aryl-4-benzoyl-imidazole; AICA, 2-aryl-imidazole-4-carboxylic amide; SMART, 4-substituted methoxylbenzoyl-aryl-thiazole; MDR, multidrug resistant; IC_{50}, 50% inhibition concentration; nM, nanomolar per liter; μM, micromolar per liter; SPA, scintillation proximity assay; SAR, structure–activity relationship; DTIC, dacarbazine; EDG, electron donating group; EWG, electron withdrawing group; Pgp, P-glycoprotein; DBU, 1,8-diazabicycloundec-7-ene; SRB, sulforhodamine B assay; DMSO, dimethyl sulfoxide; DMF, dimethylformamide; THF, tetrahydrofuran; TMS, tetramethylsilane; NMR, nuclear magnetic resonance; SEM, standard error of the mean; rt, room temperature; RP-HPLC, reverse phase-high performance liquid chromatography; ESI, electrospray ionization; LC-MS, liquid chromatography–mass spectrometry; PDB, Protein Data Bank; TLC, thin layer chromatography.

modified from an amide in the AICA derivatives to a carbonyl group in ABIs. For the C ring, different substituted phenyls were introduced. We show that replacing the thiazole ring with an imidazole ring retained the antiproliferative activity with significantly improved water solubility. Mechanism of action studies indicated that the ABI analogues work by competitively binding to the colchicine binding site in the α/β tubulin dimer and disrupting tubulin polymerization. However, unlike existing drugs targeting tubulin such as paclitaxel and vinblastine, the ABI compounds are equally effective against multidrug-resistant cancer cells, therefore, they hold great promise as potential drugs to treat resistant cancer.

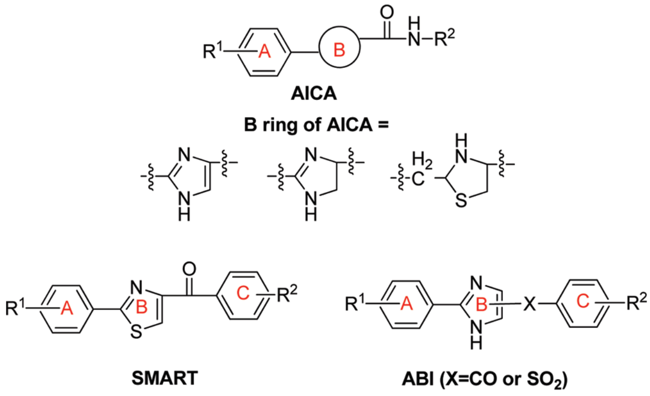

Figure 1. General structures of AICA, SMART, and ABI.

Chemistry

The general synthesis of the ABI analogues is outlined in Schemes 1−3. First, a series of imidazolines (**7b−x**) was synthesized by reacting the appropriately substituted benzaldehyde with ethylene diamine in the presence of iodine and potassium carbonate (Scheme 1).[7] Second, the imidazoline (**7b−x**) was oxidized to the corresponding imidazole catalyzed by diacetoxyiodobenzene.[7] Compounds **2b** and **2x** were generated by this method. However, it was not successful when

Scheme 1[a]

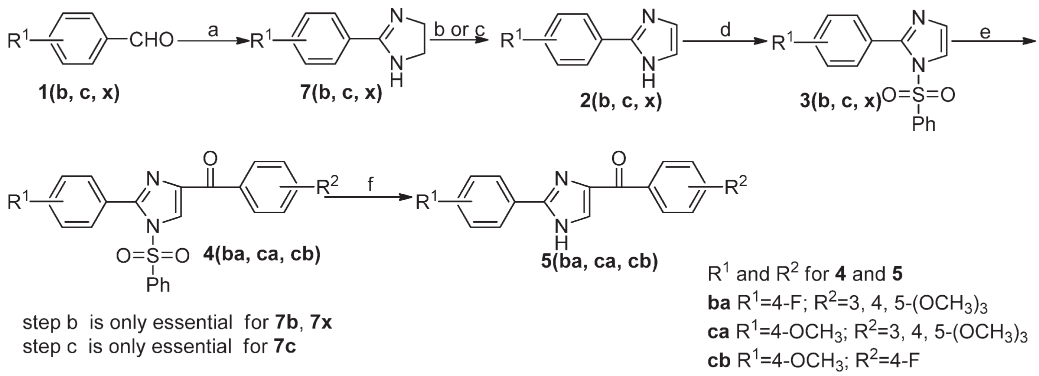

[a] Reagents and conditions: (a) *t*-BuOH, I_2, ethylenediamine, K_2CO_3, reflux; (b) PhI $(OAc)_2$, K_2CO_3, DMSO; (c) DBU, $CBrCl_3$, DMF; (d) NaH, $PhSO_2Cl$, THF, 0 °C−rt; (e) *t*-BuLi, substituted benzoyl chloride, THF, −78 °C; (f) Bu_4NF, THF, rt.

Scheme 2[a]

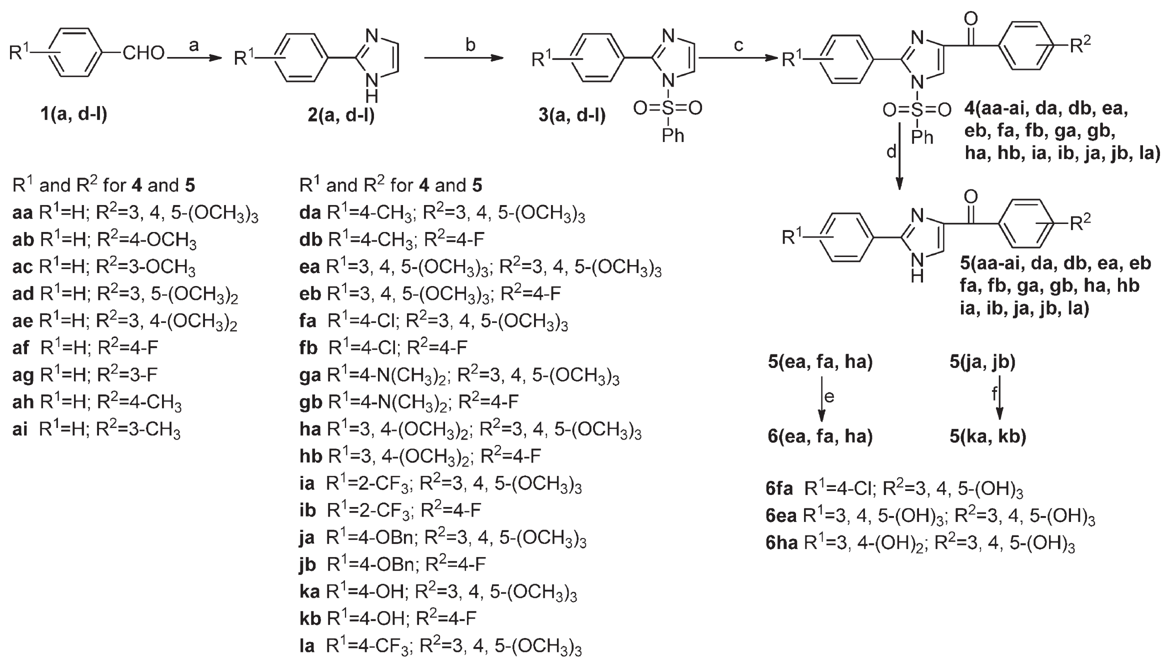

[a] Reagents and conditions: (a) NH_4OH, oxalaldehyde, ethanol, rt; (b) NaH, $PhSO_2Cl$, THF, 0 °C−rt; (c) *t*-BuLi, substituted benzoyl chloride, THF, −78 °C; (d) Bu_4NF, THF, rt; (e) BBr_3, CH_2Cl_2; (f) c-HCl, AcOH, reflux.

Scheme 3[a]

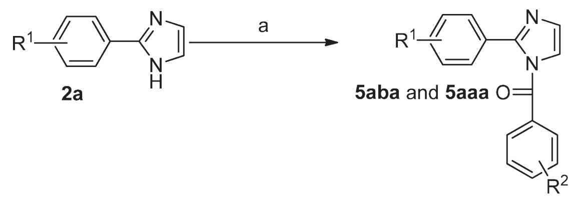

R^1 and R^2 for
5aba R^1=H; R^2=4-OCH_3
5aaa R^1=H; R^2=3, 4, 5-$(OCH_3)_3$

[a] Reagents and conditions: (a) NaH, substituted benzoyl chloride, THF.

Table 1. In Vitro Growth Inhibitory Effects of Compounds without A Ring Substitutions

Structure	ID	R	IC_{50} ± SEM (μM)						
			A375	B16-F1	WM164	LNCaP	PC-3	Du 145	PPC-1
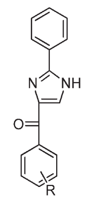	**5aa**	3,4,5-$(OMe)_3$	0.16±0.02	0.12±0.01	0.10±0.01	0.15±0.02	0.29±0.04	0.20±0.03	0.13±0.01
	5ab	4-OMe	>10	>10	>10	>10	>10	>10	>10
	5ac	3- OMe	>10	>10	>10	>10	>10	>10	>10
	5ad	3, 5-$(OMe)_2$	2.8±0.5	5.4±0.8	2.1±0.4	3.6±0.3	3.2±0.5	2.6±0.3	2.1±0.2
	5ae	3, 4-$(OMe)_2$	>10	>10	>10	>10	>10	>10	>10
	5af	4-F	0.58±0.07	0.93±0.1	0.63±0.09	0.61±0.08	2.1±0.3	0.85±0.1	0.57±0.1
	5ag	3-F	>10	>10	>10	>10	>10	>10	>10
	5ah	4-Me	>10	>10	>10	>10	>10	>10	>10
	5ai	3-Me	>10	>10	>10	>10	>10	>10	>10
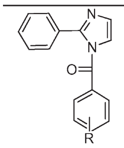	**5aba**	4-OMe	>10	>10	>10	>10	>10	>10	>10
	5aaa	3,4,5-$(OMe)_3$	>10	>10	>10	>10	>10	>10	>10
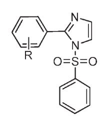	**3a**	H	>10	>10	>10	>10	>10	>10	>10
	3x	4-NO2	>10	>10	>10	>10	>10	>10	>10
	3j	4-OBn	>10	>10	>10	>10	>10	>10	>10

applied to other analogues with different substitutions in the A ring. Consequently, bromotrichloromethane and DBU were used as the oxidizing agents to convert imidazoline to the corresponding imidzaole.[8] Although compound **2c** was produced by this means, this method was discontinued because of poor yield (<5%). Other attempts were also made by using different oxidizing agents including the activated carbon$-O_2$ system[9] and palladium$-$carbon system,[10] but neither of these methods gave a satisfactory yield (<2%). In our efforts to find an alternative way to construct the imidazole ring, we tried starting with iminoether[11] but abandoned this approach because of the multistep synthesis. Finally, a simple, one-step synthesis of the key intermediate (**2a**$-$**k**) was found (Scheme 2) by reacting the appropriate benzaldehyde (**1a**$-$**h**) in ethanol with oxalaldehyde and ammonia hydroxide to construct the imidazole ring system (**2a**$-$**k**).[12] The yield from this method was not high (approximately 20$-$40%), but it was acceptable to conduct the subsequent reactions. 2-Aryl-1*H*-imidazole (**2a**$-$**k**) was then converted to the *N*-phenylsulfonyl protected 2-aryl-imidazoles (**3a**$-$**k**) by treating with phenylsulfonyl chloride and sodium hydride in THF.[13] Compounds **3a**$-$**k** were coupled with an appropriately substituted benzoyl chloride in the presence of *tert*-butyl lithium to obtain the aryl (2-aryl-1-(phenylsulfonyl)-1*H*-imidazol-4-yl) methanone (**4ab**$-$**jb**).[13] Removing the protecting group from **4ab**$-$**jb** by tetrabutylammonium fluoride in THF gave the desired ABI agents (**5aa**$-$**hb**).[13] Compounds **5aba** and **5aaa** were straightforwardly prepared based on the reaction of 2-phenyl-1*H*-imidazole (**2a**) with an appropriate benzoyl chloride following a known method (Scheme 3).[14] Compounds **6ea**, **6fa**, and **6ha** were afforded by treating **5ea**, **5fa**, and **5ha**, respectively, with BBr_3 to remove the methyl groups. Likewise, debenzylation of **5ja** and **5jb** by concentrated HCl provided **5ka** and **5kb**, respectively.

Biological Results and Discussion

We first assessed the in vitro antiproliferative activities of these compounds using three melanoma cell lines (one murine melanoma cell line, B16$-$F1, and two human metastatic melanoma cell lines, A375 and WM-164) and four human prostate cancer cell lines (LNCaP, PC-3, Du 145, and PPC-1). The results are summarized in Tables 1$-$4.

Effects of Substitutions on the C Ring (Table 1). A variety of compounds (**5aa**$-$**5ai**) with an unsubstituted A-ring and different C-ring substituents generally showed moderate activity (Table 1), with IC_{50} values in the μM range (unless specified, the IC_{50} value for a specific compound discussed in the text is referred to as an average of all seven cell lines). The most potent compound of this series was **5aa**, with an average IC_{50} value of 160 nM. The removal of one of the methoxy groups from the 3,4,5-trimethoxy on the C ring (**5ad**, **5ae**) led to a significant loss of activity (IC_{50} > 10 μM for **5ae** and an IC_{50} of 3.1 μM for **5ad**). This finding is consistent with results

Table 2. In Vitro Growth Inhibitory Effects of Compounds with Substitutions on A Ring[a]

Structure	ID	R^1	R^2	$IC_{50} \pm$ SEM (nM)						
				A375	B16-F1	WM164	LNCaP	PC-3	Du 145	PPC-1
	5ba	4-F	3,4,5-$(OMe)_3$	205±19	320±41	73±8	98±2	169±12	132±24	81±1
	5ca	4-OMe	3,4,5-$(OMe)_3$	30±5	108±12	31±4	31±1	45±1	48±0.5	34±0.3
	5cb	4-OMe	4-F	31±5	63±7	28±3	28±2	31±2	41±38	29±1
	5da	4-Me	3,4,5-$(OMe)_3$	9±2	46±5	8±2	12±1	9±0.4	15±0.5	11±0.1
	5db	4-Me	4-F	142±13	222±10	156±19	45±2	65±3	78±5	54±1
	5db-HCl			108±11	297±23	112±9	ND	ND	ND	ND
	5ea	3,4,5-$(OMe)_3$	3,4,5-$(OMe)_3$	4800	>10000	>10000	>10000	>10000	>10000	>10000
	5eb	3,4,5-$(OMe)_3$	4-F	>10000	>10000	>10000	>10000	>10000	>10000	>10000
	5fa	4-Cl	3,4,5-$(OMe)_3$	43±5	168±14	26±3	24±1	35±1	36±0.4	26±0.2
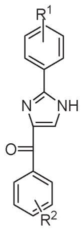	**5fb**	4-Cl	4-F	52±4	73±6	74±9	49±2	81±2	65±1	52±1
	6fa	4-Cl	3,4,5-$(OH)_3$	3900	1810	2100	10000	10000	10000	>10000
	5ga	4-$N(Me)_2$	3,4,5-$(OMe)_3$	82±9	361±29	80±11	58±2	92±4	95±1	67±0.7
	5gb	4-$N(Me)_2$	4-F	56±7	129±11	62±8	57±6	81±3	72±0.4	45±0.3
	5ha	3,4-$(OMe)_2$	3,4,5-$(OMe)_3$	113±14	1400±200	191±18	121±10	203±7	168±15	117±1
	5hb	3,4-$(OMe)_2$	4-F	10000	4210	1400	2533	10000	10000	2172±48
	5ia	2-CF_3	3,4,5-$(OMe)_3$	>10000	>10000	>10000	>10000	>10000	>10000	>10000
	5ib	2-CF_3	4-F	>10000	>10000	>10000	>10000	>10000	>10000	>10000
	6ea	3,4,5-$(OH)_3$	3,4,5-$(OH)_3$	>10000	>10000	>10000	>10000	>10000	>10000	>10000
	5ja	4-OBn	3,4,5-$(OMe)_3$	5200	10000	5500	2786	10000	10000	2844
	5jb	4-OBn	4-F	93±8	117±16	90±12	44±7	79±0.4	60±3	43±0.2
	5ka	4-OH	3,4,5-$(OMe)_3$	1600	2400	1800	ND	ND	ND	ND
	5kb	4-OH	4-F	10000	>10000	>10000	10000	>10000	>10000	>10000
	5la	4-CF_3	3,4,5-$(OMe)_3$	163±10	468±25	175±16	134±6	127±7	174±31	110±3
	6ha	3,4-$(OH)_2$	3,4,5-$(OH)_3$	>10000	>10000	>10000	>10000	>10000	>10000	>10000
	Colchicine			20±3	29±5	ND	16±4	11±1	10±2	20±1

[a] ND: not determined.

from SMART compounds in which the 3,4,5-trimethoxy substituted compound was most potent. It should be noted that the compound with 4-fluoro on the C ring (**5af**) also showed relatively good activity (IC_{50} = 0.91 μM), a finding that has an important implication because replacing the trimethoxy moiety with a 4-fluoro group may provide good activity and improved metabolic stability. Interestingly, the position of the fluorine on the C ring was critical for activity because a shift from 4-fluoro to 3-fluoro resulted in a total loss of activity (IC_{50} > 10 μM for **5ag** compared with 0.91 μM for **5af**). This result suggested that a potential hydrogen bond donor is present close to the 4-position of this ring. As shown in the molecular modeling studies below, this hydrogen bond donor is likely to be the thiol group in Cys-241 in loop 7 of the β-substituent in α/β-tubulin dimer. Other substituents such as methoxy and methyl at the 3 or 4 position on the C ring (**5ab**, **5ac**, **5ah**, **5ai**) were also evaluated, but none showed good activity (IC_{50} > 10 μM). As clearly indicated in Table 1, the positions of the A and C rings were critical. A simple shift of the C-ring moiety from position 4 to position 1 in the imidazole ring (B ring) resulted in total loss of activity (IC_{50} > 10 μM for **5aba**, **5aaa**, **3a**, **3x**, **3j**). This result is consistent with recent reports in which the position of the aryl group was found to be important for antiproliferative activity.[15,16] Bellina and co-workers reported potent antitumor activity for a series of 1,5- and 1,2-diaryl-1*H*-imidazole analogues. While the 1,5-diaryl-imidazole analogues have nanomolar activity, a simple shift of the diaryl substitution from the 1,5-position to 1,2-position resulted in significantly lower activity down to the micromolar range.[15] Similarly, Wang and co-workers reported that 4,5-disubstituted and 1,5-disubstituted imidazoles are much more active than the corresponding 1,2-disubstituted imidazoles.[16]

Effects of Substitutions on the A Ring (Table 2). Because compounds with 3,4,5-trimethoxy and 4-fluoro substitutions on the C ring showed good activity, a series of compounds was synthesized with fixed substitutions on the C ring (4-fluoro or 3,4,5-trimethoxy) and different substitutions on the A ring (Table 2). These compounds demonstrated excellent antiproliferative activity with IC_{50} values as low as 8.0 nM on the WM164 cell line (**5da**). In general, compounds incorporating a single substituent on the para-position of the A ring were more potent as can be seen from the activities of **5ca**, **5cb**, **5da**, **5db**, **5fa**, **5fb**, **5ga**, and **5gb** (IC_{50} = 7.9−110 nM). **5db**-HCl salt (IC_{50} = 172 nM) showed slightly diminished activity compared with the corresponding free base **5db** (IC_{50} = 109 nM). Compound **5fb** (IC_{50} = 63.7 nM), which has a single halogen substituent in the para-position of the A and C rings, demonstrated potency and was devoid of a methoxy moiety. Compounds with 3,4,5-trimethoxy substituents on the A ring lost activity completely (IC_{50} > 10 μM for **5ea**, **5eb**), suggesting very different binding environments near the A ring and C

Table 3. In Vitro Growth Inhibitory Effects of Compounds with Protection on B Ring

Structure	ID	R^1	R^2	IC_{50} ± SEM (nM)						
				A375	B16-F1	WM164	LNCaP	PC-3	Du 145	PPC-1
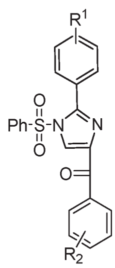	**4ab**	H	4-OMe	>10000	>10000	>10000	>10000	>10000	>10000	>10000
	4ac	H	3-OMe	>10000	>10000	>10000	>10000	>10000	>10000	>10000
	4ah	H	4-Me	>10000	>10000	>10000	>10000	>10000	>10000	>10000
	4af	H	4-F	630±72	946±86	596±61	573	2233	846	575
	4ag	H	3-F	>10000	>10000	>10000	>10000	>10000	>10000	>10000
	4cb	4-OMe	4-F	36±5	71±8	43±6	31±2	33±2	52±3	32±0.7
	4db	4-Me	4-F	113±14	287±31	107±14	55±3	80±1	80±1	57±1
	4ea	3,4,5-$(OMe)_3$	3,4,5-$(OMe)_3$	>10000	>10000	>10000	>10000	>10000	>10000	>10000
	4eb	3,4,5-$(OMe)_3$	4-F	3840	>10000	>10000	>10000	>10000	>10000	>10000
	4fb	4-Cl	4-F	88±9	107±12	70±6	48±1	76±2	64±1	54±1
	4ga	4-$N(Me)_2$	3,4,5-$(OMe)_3$	162±13	1200±90	308±32	62±2	93±6	99±2	72±0.4
	4gb	4-$N(Me)_2$	4-F	55±7	242±26	56±4	56±6	83±3	74±0.5	48±0.3
	4ha	3,4-$(OMe)_2$	3,4,5-$(OMe)_3$	192±15	970±68	139±15	114±6	197±9	144±29	117±2
	4hb	3,4-$(OMe)_2$	4-F	960±59	2000±400	1400±30	1915±77	10000	3312	1441±49
	4ia	2-CF_3	3,4,5-$(OMe)_3$	>10000	>10000	>10000	>10000	>10000	>10000	>10000
	4ib	2-CF_3	4-F	>10000	>10000	>10000	>10000	>10000	>10000	>10000
	4jb	4-OBn	4-F	64±7	110±15	48±5	35±1	75±0.5	58±1	38±0.2

ring. Removal of the 5-methoxy substituent from the A-ring improved activity significantly (IC_{50} = 330 nM and > 10 μM for **5ha**, **5ea**, respectively). Demethylation of the 3,4,5-trimethoxy decreased activity sharply from 43 nM (**5fa**) to 3.89 μM (**6fa**). Similar results were observed for **6ea**, **5ka**, **5kb**, and **6ha** due to the demethylation of subsituents on either the A or C ring. Electron-donating groups (4-methoxy, 4-dimethylamino, 4-methyl) and electron-withdrawing groups (4-chloro, 4-trifluoromethyl) on the A ring did not show substantial differences in activity. The introduction of a trifluoromethyl group at the para-position of the A ring (IC_{50} = 193 nM for **5la**) led to a 12-fold decrease of activity compared with compound **5da** (IC_{50} = 15.7 nM), which has a methyl group at the para-position. In addition, a shift of the trifluoromethyl group from para to ortho position in the A ring caused complete loss of activity (IC_{50} > 10 μM for **5ia**, **5ib**), consistent with the results with other substituents. The presence of a benzoloxy group at the para-position of the A ring (IC_{50} = 75 nM for **5jb**) resulted in a 440-fold increase in activity when compared with the *para*-hydroxy compound **5kb** (IC_{50} = 33 μM). It is worthwhile to note that compound **5jb**, with the 4-fluoro in the C ring, has better activity than does its counterpart **5ja**, which has a 3,4,5-trimethoxy group in the C ring (IC_{50} is 75 nM for **5jb** and 7.3 μM for **5ja**).

Effects of Additional Substitutions on the B Ring (Table 3). Interestingly, some of the compounds with a phenylsulfonyl protection group attached to the nitrogen of the imidazole ring (**4cb**, **4db**, **4fb**, **4ga**, **4gb**, **4ha**, **4jb**) were also very active, with IC_{50} in the nM range (Table 3). Generally, the activities of these compounds are comparable to their corresponding unprotected counterparts as exemplified by comparing the activities of **4cb** (43 nM), **4db** (111 nM), **4fb** (72 nM), **4ga** (285 nM), **4gb** (87 nM), **4ha** (268 nM), and **4jb** (61 nM) with their corresponding unprotected counterparts **5cb** (36 nM), **5db** (109 nM), **5fb** (64 nM), **5ga** (131 nM), **5gb** (72 nM), **5ha** (330 nM), and **5jb** (75 nM). Other compounds (**4ab**−**4ag**, **4ea**, **4eb**, **4hb**, **4ia**, and **4ib**, 1−50 μM) were generally much less active, also in line with their counterparts (**5ab-5ag**, **5ea**, **5eb**, **5hb**, **5ia**, and **5ib**, 1−50 μM). The comparable activity of these N-protected compounds with their unprotected counterparts may suggest that they may have similar binding interactions to their target. It is possible that the N-protection group does not contribute significantly to the binding for these compounds, as we will see from the molecular modeling studies for compounds **4cb** and **5cb**.

ABI Compounds Are Effective against Multidrug Resistant Melanoma Cells (Table 4). Pgp-mediated drug efflux represents a major mechanism for cancer cells to prevent the build up of effective anticancer intracellular drug concentrations. We compared the activity of the ABI compounds against multidrug resistant melanoma cells (MDA-MB-435/LCCMDR1) and their parental nonresistant cancer cells (MDA-MB-435). Although MDA-MB-435 was originally designated as a breast cancer cell line, it has been shown definitively to originate from the M14 melanoma cell line.[17−19] This pair of cell lines have been well validated and widely used to assess abilities of drugs overcoming Pgp-mediated MDR.[20−23] Compounds **5cb**, **4cb**, and **4fb**, together with other tubulin-targeting agents including colchicine, paclitaxel, and vinblastine, were tested on both the MDR melanoma cell line and its parental melanoma cell line (Table 4). Compounds **5cb**, **4cb**, and **4fb** had much better resistance indices (1.3 for **5cb**, 0.8 for **4cb**, 0.7 for **4fb**) than colchicine (65.8), paclitaxel (69.3), and vinblastine (27.5). Although colchicine, paclitaxel, and vinblastine showed excellent activity in nonresistant melanoma cell lines (0.5−10 nM), these compounds were significantly less potent in the MDR melanoma cell line (277−658 nM). In contrast, **5cb**, **4cb**, and **4fb** had essentially equivalent potency on both MDR (30, 30, and 35 nM for **5cb**, **4cb**, and **4fb**, respectively) and nonresistant melanoma cellines (24, 38, and 50 nM for **5cb**, **4cb**, and **4fb**, respectively).

ABI Compound 5cb is Highly Active in Vivo. To evaluate efficacy of ABI analogues in vivo, we tested the antitumor activity of compound **5cb** on mice melanoma B16−F1 xenograph. DTIC, the gold standard in malignant melanoma treatment, was used as a positive control.[24] Compound

5cb was selected for the in vivo studies because it is more stable compared with compound **5da**; although **5da** (IC_{50} = 15.7 nM) showed higher in vitro potency than **5cb** (IC_{50} = 35 nM), it has been proven to be susceptible to demethylation due to the presence of the 3,4,5-trimethoxy moiety on the C-ring.[25] Twenty female C57/BL mice were divided into four groups: a vehicle control group, a DTIC (60 mg/kg) treatment group,[24] a **5cb** (10 mg/kg) treatment group, and a **5cb** (30 mg/kg) treatment group. Each mouse was injected with 0.5 million B16−F1 melanoma cells subcutaneously. Seven days after tumor inoculation, treatment started with each compound injected intraperitoneally daily (Figure 2). Tumor volume was significantly ($p < 0.05$) reduced 47%, 51%, and 73% for **5cb** (10 mg/kg), DTIC (60 mg/kg), and **5cb** (30 mg/kg), respectively, after 14 days of treatment. No significant weight loss was observed in any of the treatment groups during the experiment.

Table 4. In Vitro Growth Inhibitory Effects of the ABI Compounds in Comparison to Other Anticancer Drugs on Multidrug-Resistant Melanoma Cell Line (MDR cell) and the Matching Sensitive Parent Cell Line (Normal Melanoma Cell)

	IC_{50} ± SEM (nM) (n = 3)		
compd ID	MDA-MB-435	MDA-MB-435/LCC6MDR1	resistance index[a]
5cb	24 ± 2	30 ± 4	1.3
4cb	38 ± 3	30 ± 2	0.8
4fb	50 ± 6	35 ± 3	0.7
paclitaxel	4 ± 1	277 ± 41	69.3
vinblastine	0.4 ± 0.1	11 ± 1	27.5
colchicine	10 ± 1	658 ± 50	65.8

[a] Resistance indexes were calculated by dividing IC_{50} values on multidrug-resistant cell line MDA-MB-435/LCC6MDR1 by IC_{50} values on the matching sensitive parental cell line MDA-MB-435.

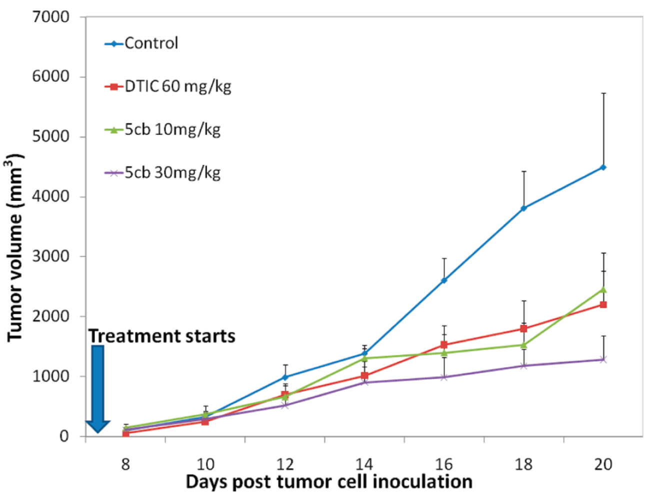

Figure 2. In vivo study of **5cb** against B16−F1 melanoma tumors in C57/BL mice.

ABI Analogues Have Significantly Higher Water Solubility than SMART Analogues (Table 5). We compared the HPLC retention times of ABI compound **5ga** (1.5 min) and its corresponding SMART analogue (**SMART-1**, 2.2 min) using 80/20 methanol/water mobile phase at 1 mL/min flow rate and a reversed phase column, indicating that the imidazole derivative was more hydrophilic than its corresponding SMART analogue. The calculated log P values for ABI compound **5ga** and the corresponding SMART analogue (**SMART-1**) were approximately 2.9 and 4.4, respectively. We also determined the aqueous solubility of compound **5ga** and its corresponding SMART analogue (**SMART-1**) using a miniturized shake-flask method and LC-MS/MS quantification. The aqueous solubility of compound **5ga** was 48.9 and 11.3 μg/mL in buffer pH7.0 and water, respectively, or about 50 and 10 times greater than its SMART counterpart, **SMART-1** (0.909 and 0.83 μg/mL in buffer pH7.0 and water, respectively). Combretastatin A4 (CA-4) and paclitaxel were used as positive controls because of their well-established antitumor activity and extensive studies on these two compounds. It is also very interesting to compare the aqueous solubility of ABI analogues with CA-4 and paclitaxel because they all target tubulin polymerization (see below for mechanism studies for ABI analogues). The aqueous solubility determined in this parallel experiment was 1.04 μg/mL in buffer pH7.0 and 2.83 μg/mL in water for CA-4, and 0.137 μg/mL in buffer pH 7.0 and 0.021 μg/mL in water for paclitaxel. Collectively, these results indicate that **5ga** and presumably other ABI analogues, due to the high structural similarity with **5ga**, have much higher aqueous solubility than their SMART counterparts.

Mechanism of Action Studies. We hypothesized that the ABI compounds have a similar mechanism of action to the SMART compounds that involve binding to the colchicine site in tubulin α/β-heterodimer. We first performed experiments to confirm the inhibition of tubulin polymerization by

Table 5. Aqueous Solubility of ABI and Its SMART Counterpart (**SMART-1**) As Well As CA-4 and Paclitaxel

Compound name	Structure	Media	Solubility (μg/mL)	Std Dev	%CV
SMART-1	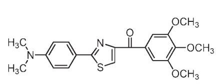	Buffer pH 7.0	0.909	0.057	6.2
		Water	0.833	0.169	20.3
ABI-5ga	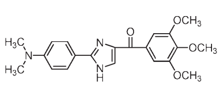	Buffer pH 7.0	48.9	5.59	11.4
		Water	11.3	1.70	15.0
Combretastatin A4	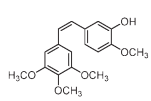	Buffer pH 7.0	1.04	0.147	14.2
		Water	2.83	0.330	11.7
Paclitaxel	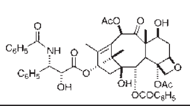	Buffer pH 7.0	0.137	0.024	17.5
		Water	0.021	0.004	20.7

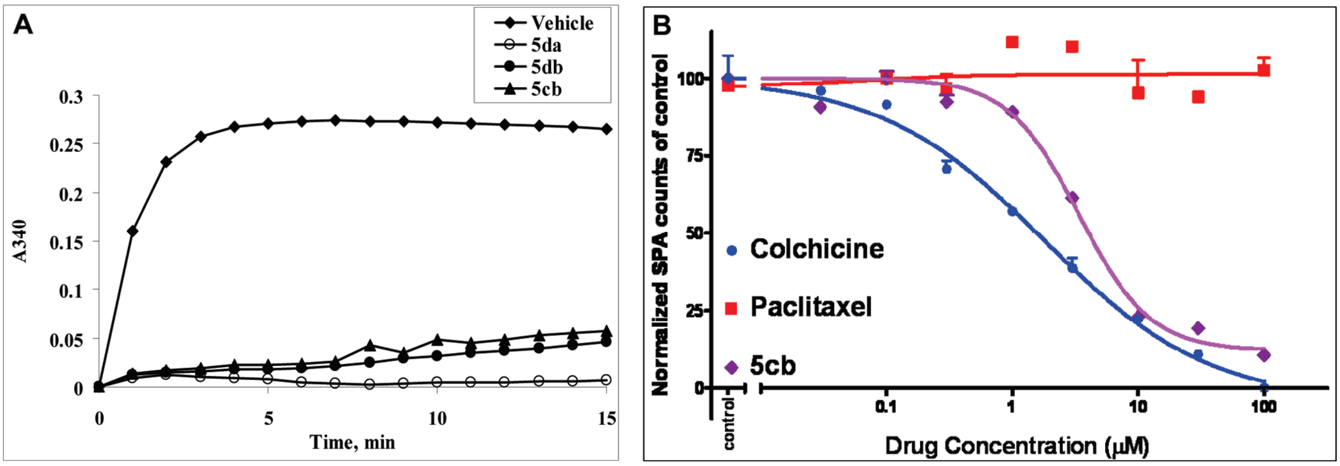

Figure 3. (A) Effect of ABI compounds on tubulin polymerization in vitro. Tubulin (0.4 mg/assay) was exposed to 10 μM ABI compounds (vehicle control, 5% DMSO). Absorbance at 340 nm was monitored at 37 °C every minute for 15 min. (B) [^{3}H]-Colchicine competition-binding scintillation proximity assay showed that ABI compounds competitively bound to tubulin colchicine binding site.

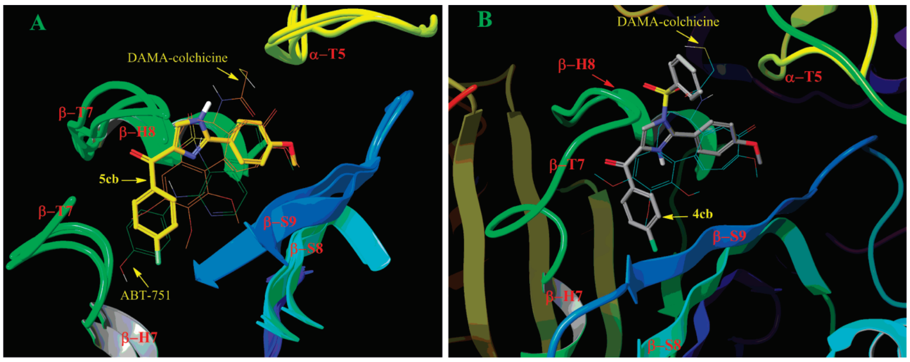

Figure 4. Proposed binding mode of ABI analogues in the colchicine binding site.

ABI compounds. Bovine brain tubulin (> 97% pure) was incubated with three potent ABI compounds, **5cb**, **5da**, and **5db**, at a concentration of 10 μM to determine the effect of these ABI compounds on tubulin polymerization (Figure 3A). Tubulin polymerization was completely inhibited by compound **5da**, while ~80% inhibition was observed during incubation with compounds **5cb** and **5db**.

Three ligand binding sites in tubulin α/β-heterodimer have been reported: paclitaxel binding site,[26] vinblastine binding site,[26,27] and colchicine binding site.[26−28] The structural similarity with the SMART compounds and the effects on tubulin polymerization prompted us to hypothesize that ABI compounds bind to the colchicine binding site in tubulin. We measured the binding affinity of compound **5cb** using ^{3}H-labeled colchicine and a competitive binding scintillation proximity assay (SPA).[29] The results confirmed the strong binding of **5cb** with a binding affinity of 3.4 ± 1.5 μM (Figure 3B). Colchicine bound tubulin with an IC_{50} value of 1.8 ± 0.5 μM under these conditions. These results clearly indicated that ABI compounds effectively inhibit tubulin polymerization, similar to the protocol SMART compounds.

Proposed Binding Mode of ABI Binding at the Colchicine Binding Site. We next investigated with molecular modeling the possible binding mode for these compounds in tubulin. Several crystal structures of the ligand−tubulin complex are available in the Protein Data Bank (PDB),[27,28,30] with the most recent one from Dorleans et al.[30] In general, the colchicine binding pocket tolerates a variety of molecular structures, which may indicate substantial conformation changes upon ligand binding. In fact, Dorleans et al. solved the crystal structures of both the empty tubulin dimer and the ligand−tubulin complex.[30] They found that, without the presence of ligand, loop 7 (T7, residues 244−251, Figure 4) in the β-monomer folds in to occupy the binding pocket, while it flips out upon ligand binding. The associated helix 7 (H7, residues 224−243) and helix 8 (H8, residues 252−260) were displaced upon ligand binding. It is conceivable that the extent to which T7 is displaced depends on the size of individual ligand. This flexibility presents a significant challenge to understand the precise binding modes for individual ligands without solving actual crystal structures. Nevertheless, careful analysis of the possible binding modes could provide some insights into the binding of different ligands.

The binding modes of **5cb** and **4cb** (stick model) are shown in parts A and B of Figure 4. For comparison, we also displayed the crystal structure complexes of ABT-751 and DAMA-colchicine (wire models) along with ABI-**5cb**/tubulin complex in Figure 4A. For clarity, only the related secondary structures forming the binding pocket in β-tubulin are shown in Figure 4A. The overall structures of **5cb**, ABT-751, and DAMA-colchine overlapped very well in the binding pocket. Several potential hydrogen bonding interactions between compound **5cb** and tubulin were identified. The carbonyl group in **5cb** was in sufficient proximity to form two hydrogen bond interactions with the backbone NH of Leu-252 in H8 and the side chain of Asp-251 in T7 of the tubulin β-monomer.

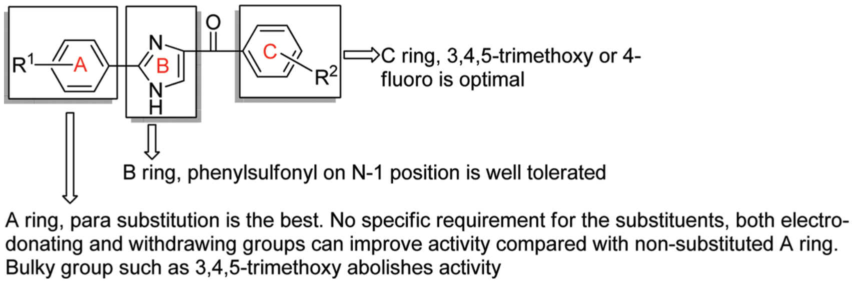

Figure 5. SAR relationship of the ABI analogues.

The *para*-fluorine substituent in the C-ring was close to the side chain of Cys241 in T7 and Tyr202 in S6, possibly forming one or two hydrogen bonds. The imidazole proton is very close and likely to form a hydrogen bond to Thr179 in T5 loop (residues 173−182) of the tubulin α-monomer (Figure 4A). Many of these interactions are consistent with literature reports with closely related ligands. Together with the hydrophobic interactions provided by the aromatic rings, the likely formation of these hydrogen bonds would contribute to the high binding affinity to the tubulin dimer, resulting in high antiproliferative potency.

The binding mode of **4cb** will be conceivably less defined because two of the three aromatic rings may occupy the binding pocket in the β-monomer while the third ring may extend toward the interface of the α/β-monomers, similar to how the side chain of DAMA-colchicine binds. Our modeling indicates that the protecting group likely extends to the tubulin dimer interface, while the A and C rings of **4cb** occupy similar binding pocket and orientation as **5cb** (Figure 4B). This may explain the similar activity between the two compounds even though **4cb** has an extra ring system. If this is true, it is possible to design new generations of ligands by properly incorporating more hydrophilic groups to further improve aqueous solubility.

Conclusions

We synthesized a set of novel 2-aryl-4-benzoyl-imidazole (ABI) derivatives that showed potent activity in a number of cancer cell lines as well as in a xenograft model. The compounds inhibited tubulin polymerization by binding to the colchicine binding site. Structure−activity relationships (SAR) (Figure 5) were investigated by introducing different substituents into the A and C rings. Compared with the earlier SMART compounds and other well-established anticancer agents such as paclitaxel and DTIC, ABI analogues showed three improvements. First, aqueous solubility was significantly improved (**5ga**, 48.9 μg/mL) compared with that of SMART analogues (**SMART-1**, 0.909 μg/mL). Compared with CA-4, which has a similar mechanism of action, **5ga** has at least 15-fold higher aqueous solubility. This is an important improvement because one general problem with drugs targeting tubulin polymerization such as paclitaxel is the poor aqueous solubility. In fact, in the ongoing clinical trial with CA-4, due to its poor aqueous solubility, its phosphate pro-drug (CA-4P) has to be used.[31] Second, compound **5cb** showed a much better resistance index (1.3) compared with colchicine (65.8), paclitaxel (69.3), and vinblastine (27.5). The fact that **5cb** can overcome multidrug resistance suggests a promising future development of more drug-like agents. Third, our in vivo study showed that compound **5cb** at a dose of 30 mg/kg gave better tumor suppression than that of DTIC at a dose of 60 mg/kg. Additional work is underway to test these compounds in other types of cancers to further optimize their efficacy.

Experimental Section

General. All reagents were purchased from Sigma-Aldrich Chemical Co., Fisher Scientific (Pittsburgh, PA), Alfa Aesar (Ward Hill, MA), and AK Scientific (Mountain View, CA) and were used without further purification. The solvents for moisture-sensitive reactions were freshly distilled, and the reactions were carried out under an argon atmosphere. Routine thin layer chromatography (TLC) was performed on aluminum-backed Uniplates (Analtech, Newark, DE). Melting points were measured with Fisher−Johns melting point apparatus (uncorrected). NMR spectra were obtained on a Varian Inova-500 spectrometer or a Bruker AX 300 (Billerica, MA) spectrometer. Chemical shifts are reported as parts per million (ppm) relative to TMS in $CDCl_3$. Mass spectra were collected on a Bruker ESQUIRE electrospray/ion trap instrument in positive and negative ion modes. The purity of the final compounds was tested via RP-HPLC on a Waters 2695 HPLC system installed with a photodiode array detector. Two RP-HPLC methods were conducted using a Supelco Ascentis 5 μM C-18 column (250 mm × 4.6 mm) at ambient temperature and a flow rate of 0.7 mL/min. HPLC1: gradient, solvent A (water) and solvent B (methanol), 0−20 min 40−100%B (linear gradient), 20−27 min 100%B. HPLC2: gradient, solvent A (water) and solvent B (methanol), 0−15 min 40−100%B (linear gradient), 15−25 min 100%B. UV detection at 254 nm. Purities of the compounds were established by careful integration of areas for all peaks detected and are reported for each compound in the following section.

General Procedure for the Preparation of 2-Aryl-1*H*-imidazole (2a−l,x). Method A (essential for only **2b**, **2x**): To a solution of 2-aryl-4, 5-dihydro-1*H*-imidazole **7** (35 mmol) in DMSO (100 mL) was added potassium carbonate (38.5 mmol) and diacetoxyiodobenzene (38.5 mmol). The reaction mixture was stirred overnight in darkness. Water was added, followed by extraction with dichloromethane. The organic layer was dried over magnesium sulfate and concentrated. The residue was subjected to flash column chromatography (hexane:ethyl acetate 3:2) to give a white solid. Yield: 30−50%. This method worked for only **2b** and **2x** but not for the other compounds for unknown reasons.

Method B (essential for only **2c**): To a solution of 2-aryl-4,5-dihydro-1*H*-imidazole **7** (50 mmol) in DMF (70 mL) was added DBU (55 mmol) and $CBrCl_3$ (55 mmol). The reaction mixture was stirred overnight, and a saturated $NaHCO_3$ (aqueous) solution was added followed by extraction with dichloromethane. The organic layer was dried over magnesium sulfate and concentrated. The residue was subjected to flash column chromatography (chloroform:methanol 50:1) to yield a white solid. Yield: 7%.

Method C (essential for **2a**, **2d−l**): To a solution of appropriate benzaldehyde **1** (100 mmol) in ethanol (350 mL) at 0 °C was added a solution of 40% oxalaldehyde in water (12.8 mL, 110 mmol) and a solution of 29% ammonium hydroxide in water (1000 mmol, 140 mL). After stirring for 2−3 days at room temperature, the reaction mixture was concentrated and the residue was subjected to flash column chromatography with dichloromethane as eluent to yield the titled compound as a yellow powder. Yield: 20−40%.

General Procedure for the Preparation of 2-Aryl-1-(phenylsulfonyl)-1*H*-imidazole (3a−l,x). To a solution of 2-aryl-1*H*-imidazole **2** (20 mmol) in anhydrous THF (200 mL) at 0 °C was added sodium hydride (60% dispersion in mineral oil, 1.2 g, 30 mmol) and stirred for 30 min. Benzenesulfonyl chloride (2.82 mL, 22 mmol) was added, and the reaction mixture was stirred overnight. After dilution by 100 mL of saturated $NaHCO_3$ solution (aqueous), the reaction mixture was extracted by ethyl acetate (500 mL). The organic layer was dried over magnesium sulfate and concentrated. The residue was purified by flash column chromatography (hexane:ethyl acetate 2:1) to give a pale solid. Yield: 40−50%.

General Procedure for the Preparation of Aryl (2-Aryl-1-(phenylsulfonyl)-1*H*-imidazol-4-yl) Methanone (4aa−ai, ba, ca, cb, da, db, ea, eb, fa, fb, ga, gb, ha, hb, ia, ib, ja, jb, la). To a solution of 2-aryl-1-(phenylsulfonyl)-1*H*-imidazole (6.0 mmol) **3** in anhydrous THF (30 mL) at −78 °C was added 1.7 M *tert*-butyl lithium in pentane (5.3 mL, 9.0 mmol) and stirred for 10 min. Appropriate substituted benzoyl chloride (7.2 mmol) was added at −78 °C and stirred for overnight. The reaction mixture was diluted with 100 mL of saturated $NaHCO_3$ solution (aqueous) and extracted by ethyl acetate (200 mL). The organic layer was dried over magnesium sulfate and concentrated. The residue was purified by flash column chromatography (hexane:ethyl acetate 4:1) to give a white solid. (Note. Due to the limited amount of starting material or the difficulty of separation, the following products formed in this step were used without further purification as a mixture for the next step: **4aa**, **4ad**, **4ae**, **4ai**, **4ba**, **4ca**, **4da**, **4fa**, **4ja**). Yield: 15%-40%.

General Procedure for the Preparation of Aryl (2-Aryl-1*H*-imidazol-4-yl) Methanone (5aa−ai, ba, ca, cb, da, db, ea, eb, fa, fb, ga, gb, ha, hb, ia, ib, ja, jb, la). To a solution of aryl (2-aryl-1-(phenylsulfonyl)-1*H*-imidazol-4-yl) methanone (2.0 mmol) **4** in THF (20.0 mL) was added 1.0 M tetrabutyl ammonium fluoride (4.0 mmol) and stirred overnight. The reaction mixture was diluted by 50 mL of saturated $NaHCO_3$ solution (aqueous) and extracted by ethyl acetate (100 mL). The organic layer was dried over magnesium sulfate and concentrated. The residue was purified by flash column chromatography (hexane:ethyl acetate 3:1) or recrystallized from water and methanol to give a white solid. Yield: 80−95%.

General Procedure for the Preparation of (2-(4-Hydroxyphenyl)-1*H*-imidazol-4-yl) (Aryl) Methanone (5ka, 5kb). To a solution of (2-(4-(benzyloxy) phenyl)-1*H*-imidazol-4-yl)(aryl) methanone **5** (**5ja** or **5jb**, 1 mmol) in AcOH(20 mL) was added concentrated HCl (2 mL) and refluxed overnight. After removing the solvent, the residue was recrystallized from dichloromethane to give the titled compound as a yellow solid. Yield: 70−85%.

General Procedure for the Preparation of Aryl (2-Phenyl-1*H*-imidazol-1-yl) Methanone (5aba, 5aaa). To a solution of 2-phenyl-1*H*-imidazole **2a** (10 mmol) in THF (20 mL) was added NaH (15 mmol) and substituted benzoyl chloride (12 mmol) at 0 °C. The reaction mixture was stirred overnight and diluted by saturated $NaHCO_3$ solution followed by extraction with ethyl acetate. The organic layer was dried over magnesium sulfate and concentrated. The residue was purified by flash column chromatography (chloroform) to give a white solid. Yield: 12−16%.

General Procedure for the Preparation of (2-Aryl-1*H*-imidazol-4-yl) (3,4,5-Trihydroxyphenyl) Methanone 6 (6ea, 6fa, 6ha). To a solution of aryl (2-aryl-1*H*-imidazol-4-yl) methanone **5** (**5ea**, **5fa**, **5ha**) (0.5 mmol) in CH_2Cl_2 (6.0 mL) was added 1.0 M of BBr_3 (2 mmol) in CH_2Cl_2 and stirred for 1 h at room temperature. Water was added to destroy excess BBr_3. The precipitated solid was filtered and recrystallized from MeOH to afford a yellow solid. Yield: 60−80%.

General Procedure for the Preparation of 2-Aryl-4,5-dihydro-1*H*-imidazole 7 (7b, 7c, 7x). To a solution of appropriate benzaldehyde **1** (60 mmol) in *t*-BuOH (300 mL) was added ethylenediamine (66 mmol) and stirred for 30 min at room temperature. Potassium carbonate (75 mmol) and iodine (180 mmol) were added to the reaction mixture sequentially, followed by stirring at 70 °C for 3 h. Sodium sulfite (Na_2SO_3) was added, and the mixture was extracted by chloroform. The organic layer was dried over magnesium sulfate and concentrated. The residue was purified by flash column chromatography (chloroform:methanol 20:1) to give a white solid. Yield: 50−60%.

General Procedure for the Preparation of Aryl (2-Aryl-1*H*-imidazol-4-yl) Methanone-HCl Salt (5db-HCl). To a solution of **5db** (0.5 mmol) in methanol (20 mL) was added 2 M solution of hydrogen chloride (5 mmol) in ethyl ether and stirred overnight at room temperature. The reaction mixture was concentrated, and the residue was washed by CH_2Cl_2 to yield the titled compound. Yield: 95%.

2-Phenyl-1*H*-imidazole (2a). Yield: 36.8%. ^{1}H NMR (500 MHz, DMSO) δ 12.52 (br, 1H), 7.95 (d, J = 7.0 Hz, 2H), 7.44 (t, J = 7.5 Hz, 2H), 7.34 (t, J = 7.0 Hz, 1H), 7.25−7.27 (m, 1H), 7.04−7.07 (m, 1H). MS (ESI): calculated for $C_9H_8N_2$, 144.1; found, 167.1 $[M + Na]^+$.

2-(4-Fluorophenyl)-1*H*-imidazole (2b). Yield: 56.5%. ^{1}H NMR (300 MHz, DMSO) δ 12.46 (br, 1 H), 7.94−7.99 (m, 2 H), 7.24−7.30 (m, 2 H), 7.00−7.03 (m, 2 H). MS (ESI): calculated for $C_9H_7FN_2$, 162.1; found, 163.0 $[M + H]^+$, 160.6 $[M - H]^-$.

2-(4-Methoxyphenyl)-1*H*-imidazole (2c). Yield: 22.2%. ^{1}H NMR (500 MHz, $CDCl_3$) δ 7.80 (d, J = 10.0 Hz, 2 H), 7.15 (s, 2 H), 3.86 (s, 3 H). MS (ESI): calculated for $C_{10}H_{10}N_2O$, 174.1; found, 175.0 $[M + H]^+$, 172.8 $[M - H]^-$.

2-(*p*-Tolyl)-1*H*-imidazole (2d). Yield: 36.1%. ^{1}H NMR (500 MHz, $CDCl_3$) δ 7.64 (d, J = 7.5 Hz, 2 H), 7.16 (d, J = 7.5 Hz, 2 H), 7.12 (s, 1 H), 7.02 (s, 1 H). MS (ESI): calculated for $C_{10}H_{10}N_2$, 158.1; found 159.0 $[M + H]^+$, 156.8 $[M - H]^-$.

2-(3,4,5-Trimethoxyphenyl)-1*H*-imidazole (2e). Yield: 26.0%. ^{1}H NMR (500 MHz, $CDCl_3$) δ 7.26 (s, 2 H), 7.08 (d, J = 1.5 Hz, 2 H), 3.86 (s, 3 H), 3.82 (s, 6 H). MS (ESI): calculated for $C_{12}H_{14}N_2O_3$, 234.1; found, 234.9 $[M + H]^+$.

2-(4-Chlorophenyl)-1*H*-imidazole (2f). Yield: 19.8%. ^{1}H NMR (500 MHz, DMSO) δ 13.60 (br, 1 H), 7.94 (d, J = 8.5 Hz, 2 H), 7.51 (d, J = 8.0 Hz, 2 H), 7.27 (s, 1 H), 7.03 (s, 1 H). MS (ESI): calculated for $C_9H_7ClN_2$, 178.0; found, 178.9 $[M + H]^+$.

4-(1*H*-Imidazol-2-yl)-*N*,*N*-dimethylaniline (2g). Yield: 16.5%. ^{1}H NMR (300 MHz, $CDCl_3$) δ 7.70 (dd, J = 7.0 Hz, 2.0 Hz, 2 H), 7.10 (s, 2 H), 6.75 (dd, J = 9.0 Hz, 2.0 Hz, 2 H), 3.02 (s, 6 H). MS (ESI): calculated for $C_{11}H_{13}N_3$, 187.1; found, 187.9 $[M + H]^+$, 185.8 $[M - H]^-$.

2-(3,4-Dimethoxyphenyl)-1*H*-imidazole (2h). Yield: 22.0%. ^{1}H NMR (500 MHz, $CDCl_3$) δ 7.52 (d, J = 1.5 Hz, 1 H), 7.27−7.28 (m, 1 H), 7.14 (s, 2 H), 6.88 (d, J = 8.0 Hz, 1 H), 3.91 (s, 3 H), 3.87 (s, 3 H). MS (ESI): calculated for $C_{11}H_{12}N_2O_2$, 204.1; found, 205.1 $[M + H]^+$, 202.8 $[M - H]^-$.

2-(2-(Trifluoromethyl)phenyl)-1*H*-imidazole (2i). Yield: 25.5%. ^{1}H NMR (500 MHz, DMSO) δ 12.31 (br, 1 H), 7.84 (d, J = 8.0 Hz, 1 H), 7.76 (t, J = 8.0 Hz, 1 H), 7.65 (t, J = 7.5 Hz, 1 H), 7.16 (br, 2 H). MS (ESI): calculated for $C_{10}H_7F_3N_2$, 212.1; found, 212.9 $[M + H]^+$, 210.7 $[M - H]^-$.

2-(4-(Benzyloxy)phenyl)-1*H*-imidazole (2j). Yield: 12.1%. ^{1}H NMR (500 MHz, $CDCl_3$) δ 7.77 (d, J = 8.5 Hz, 2 H), 7.36−7.47 (m, 5 H), 7.10−7.18 (m, 2 H), 7.06 (d, J = 9.0 Hz, 2 H), 5.13 (s, 2 H). MS (ESI): calculated for $C_{16}H_{14}N_2O$, 250.1; found, 251.1 $[M + H]^+$, 248.8 $[M - H]^-$.

2-(4-(Trifluoromethyl)phenyl)-1*H*-imidazole (2l). Yield: 26.2%. ^{1}H NMR ($CDCl_3$, 500 MHz) δ 8.03 (d, J = 8.0 Hz, 2 H), 7.66 (d, J = 8.0 Hz, 2 H), 7.25 (s, 2 H). MS (ESI) calculated for $C_{10}H_7F_3N_2$, 212.1; found, 213.1 $[M + H]^+$.

2-(4-Nitrophenyl)-1*H*-imidazole (2x). Yield: 53.7%. ^{1}H NMR (500 MHz, DMSO) δ 12.97 (br, 1 H), 8.32 (d, J = 9.0 Hz, 2 H), 8.17 (d, J = 9.0 Hz, 2 H), 7.42 (s, 1 H), 7.17 (s, 1H). MS (ESI): calculated for $C_9H_7N_3O_2$, 189.1; found, 189.9 $[M + H]^+$, 187.8 $[M - H]^-$.

2-Phenyl-1-(phenylsulfonyl)-1*H*-imidazole (3a). Yield: 50.3%. ^{1}H NMR (500 MHz, $CDCl_3$) δ 7.64−7.67 (m, 1H), 7.56 (t, *J* = 9.0 Hz, 1H), 7.32−7.48 (m, 9H), 7.12−7.16 (m, 1H). MS (ESI): calculated for $C_{15}H_{12}N_2O_2S$, 284.1; found, 307.1 [M + Na]$^+$.

2-(4-Fluorophenyl)-1-(phenylsulfonyl)-1*H*-imidazole (3b). Yield: 56.9%. ^{1}H NMR (500 MHz, $CDCl_3$) δ 7.66 (d, *J* = 2.0 Hz, 1 H), 7.58 (t, *J* = 10.0 Hz, 1 H), 7.36−7.42 (m, 6 H), 7.12 (d, *J* = 2.0 Hz, 1 H), 7.06 (t, *J* = 10.0 Hz, 2 H). MS (ESI): calculated for $C_{15}H_{11}FN_2O_2S$, 302.1; found, 300.8 [M − H]$^-$.

2-(4-Methoxyphenyl)-1-(phenylsulfonyl)-1*H*-imidazole (3c). Yield: 40.9%. ^{1}H NMR (500 MHz, $CDCl_3$) δ 7.62 (d, *J* = 5.0 Hz, 1 H), 7.56 (tt, *J* = 15.0 Hz, 5.0 Hz, 1 H), 7.32−7.43 (m, 6 H), 7.10 (d, *J* = 5.0 Hz, 1 H), 6.88 (dt, *J* = 16.0 Hz, 6.0 Hz, 2 H), 3.87 (s, 3 H). MS (ESI): calculated for $C_{16}H_{14}N_2O_3S$, 314.1; found, 337.1 [M + Na]$^+$, 312.9 [M − H]$^-$.

1-(Phenylsulfonyl)-2-(*p*-tolyl)-1*H*-imidazole (3d). Yield: 46.6%. ^{1}H NMR (500 MHz, $CDCl_3$) δ 7.63 (d, *J* = 1.0 Hz, 1 H), 7.55 (t, *J* = 8.0 Hz, 1 H), 7.42 (d, *J* = 8.0 Hz, 2 H), 7.35 (t, *J* = 7.5 Hz, 2 H), 7.27−7.29 (m, 2 H), 7.16 (d, *J* = 7.5 Hz, 2 H), 7.10 (s, 1 H), 2.41 (s, 3 H). MS (ESI): calculated for $C_{16}H_{14}N_2O_2S$, 298.1; found, 321.1 [M + Na]$^+$.

1-(Phenylsulfonyl)-2-(3,4,5-trimethoxyphenyl)-1*H*-imidazole (3e). Yield: 55.7%. ^{1}H NMR (500 MHz, $CDCl_3$) δ 7.68 (d, *J* = 1.5 Hz, 1 H), 7.55 (t, *J* = 7.0 Hz, 1 H), 7.42 (d, *J* = 7.5 Hz, 2 H), 7.35 (t, *J* = 8.5 Hz, 2 H), 7.11 (d, *J* = 1.5 Hz, 2 H), 6.60 (s, 1 H), 3.90 (s, 3 H), 3.79 (s, 6 H). MS (ESI): calculated for $C_{18}H_{18}N_2O_5S$, 374.1; found, 397.1 [M + Na]$^+$.

2-(4-Chlorophenyl)-1-(phenylsulfonyl)-1*H*-imidazole (3f). Yield: 54.9%. ^{1}H NMR (500 MHz, $CDCl_3$) δ 7.65 (d, *J* = 2.0 Hz, 1 H), 7.58 (t, *J* = 7.5 Hz, 1 H), 7.43 (d, *J* = 8.5 Hz, 2 H), 7.38 (t, *J* = 8.0 Hz, 2 H), 7.34−7.36 (m, 4 H), 7.12 (d, *J* = 1.5 Hz, 1 H). MS (ESI): calculated for $C_{15}H_{11}ClN_2O_2S$, 318.0; found, 341.0 [M + Na]$^+$.

***N*,*N*-Dimethyl-4-(1-(phenylsulfonyl)-1*H*-imidazol-2-yl) aniline (3g).** Yield: 48.3%. ^{1}H NMR (300 MHz, $CDCl_3$) δ 7.59 (d, *J* = 2.0 Hz, 1 H), 7.55 (t, *J* = 8.0 Hz, 1 H), 7.45 (d, *J* = 7.5 Hz, 2 H), 7.28−7.38 (m, 4 H), 7.07 (d, *J* = 2.0 Hz, 1 H), 6.68 (d, *J* = 8.5 Hz, 2 H), 3.04 (s, 3 H). MS (ESI): calculated for $C_{17}H_{17}N_3O_2S$, 327.1; found, 350.0 [M + Na]$^+$, 325.9 [M − H]$^-$.

2-(3, 4-Dimethoxyphenyl)-1-(phenylsulfonyl)-1*H*-imidazole (3h). Yield: 60.3%. ^{1}H NMR (500 MHz, $CDCl_3$) δ 7.64 (d, *J* = 7.0 Hz, 1 H), 7.55 (t, *J* = 7.5 Hz, 1 H), 7.40 (dd, *J* = 8.5 Hz, 1.5 Hz, 2 H), 7.35 (t, *J* = 8.0 Hz, 2H), 7.09 (d, *J* = 2.0 Hz, 1 H), 7.02 (dd, *J* = 8.0 Hz, 2.0 Hz, 1 H), 6.89 (d, *J* = 1.5 Hz, 1 H), 6.86 (d, *J* = 8.0 Hz, 1 H), 3.95 (s, 3 H), 3.81 (s, 3 H). MS (ESI): calculated for $C_{17}H_{16}N_2O_4S$, 344.1; found, 367.0 [M + Na]$^+$.

1-(Phenylsulfonyl)-2-(2-(trifluoromethyl) phenyl)-1*H*-imidazole (3i). Yield: 58.6%. ^{1}H NMR (500 MHz, $CDCl_3$) δ 7.64−7.67 (m, 2 H), 7.61−7.63 (m, 3 H), 7.40−7.46 (m, 5 H), 7.16 (d, *J* = 1.5 Hz, 1 H). MS (ESI): calculated for $C_{16}H_{11}F_3N_2O_2S$, 352.1; found, 353.1 [M + H]$^+$.

2-(4-(Benzyloxy)phenyl)-1-(phenylsulfonyl)-1*H*-imidazole (3j). Yield: 62.0%; mp 102−104 °C. ^{1}H NMR (500 MHz, $CDCl_3$) δ 7.56 (d, *J* = 1.0 Hz, 1 H), 7.46 (t, *J* = 8.0 Hz, 1 H), 7.20−7.40 (m, 11 H), 7.03 (d, *J* = 1.0 Hz, 1H), 6.89 (t, *J* = 8.0 Hz, 2 H), 5.08 (s,2 H). MS (ESI): calculated for $C_{22}H_{18}N_2O_3S$, 390.1; found, 413.1 [M + Na]$^+$. HPLC2: t_R 18.22 min, purity 95.9%.

1-(Phenylsulfonyl)-2-(4-(trifluoromethyl)phenyl)-1*H*-imidazole (3l). Yield: 36.7%. ^{1}H NMR ($CDCl_3$, 500 MHz) δ 7.75 (d, *J* = 2.0 Hz, 1 H), 7.69 (d, *J* = 8.0 Hz, 2 H), 7.65 (t, *J* = 8.0 Hz, 1 H), 7.60 (d, *J* = 8.0 Hz, 2 H),, 7.48 (d, *J* = 7.5 Hz, 2 H), 7.43 (t, *J* = 8.0 Hz, 2 H), 7.22 (d, *J* = 2.0 Hz, 1 H). MS (ESI) calcd for $C_{16}H_{11}F_3$-N_2O_2S, 352.1; found, 553.1 [M + H]$^+$..

2-(4-Nitrophenyl)-1-(phenylsulfonyl)-1*H*-imidazole (3x). Yield: 50%; mp 145−147 °C. ^{1}H NMR (500 MHz, DMSO) δ 8.28 (d, *J* = 8.5 Hz, 2 H), 8.03 (d, *J* = 1.5 Hz, 1 H), 7.78 (t, *J* = 7.5 Hz, 1 H), 7.64−7.68 (m, 4H), 7.60 (t, *J* = 8.0 Hz, 2 H), 7.30 (d, *J* = 1.5 Hz, 1 H). MS (ESI): calculated for $C_{15}H_{11}N_3O_4S$, 329.1; found, 352.0 [M + Na]$^+$, 327.9 [M − H]$^-$. HPLC2: t_R 14.87 min, purity 98.8%.

2-(4-Nitrophenyl)-4,5-dihydro-1*H*-imidazole (7x). Yield: 70.3%. ^{1}H NMR (500 MHz, $CDCl_3$) δ 8.30 (d, *J* = 9.0 Hz, 2 H), 7.98 (d, *J* = 8.5 Hz, 2 H), 3.88−3.95 (m, 4 H). MS (ESI): calculated for $C_9H_9N_3O_2$, 191.1; found, 191.9 [M + H]$^+$, 189.7 [M − H]$^-$.

2-(4-Fluorophenyl)-4,5-dihydro-1*H*-imidazole (7b). Yield: 60.2%. ^{1}H NMR (500 MHz, $CDCl_3$) δ 7.80 (q, *J* = 7.0 Hz, 2 H), 7.11 (d, *J* = 10.0 Hz, 2 H), 3.82 (br, 4 H). MS (ESI): calculated for $C_9H_9FN_2$, 164.1; found, 165 [M + H]$^+$.

2-(4-Methoxyphenyl)-4,5-dihydro-1*H*-imidazole (7c). Yield: 56.9%. ^{1}H NMR (500 MHz, $CDCl_3$) δ 7.84 (d, *J* = 8.5 Hz, 2 H), 6.94 (d, *J* = 9.0 Hz, 2 H), 3.87 (s, 3 H), 3.85 (br, 4 H). MS (ESI): calculated for $C_{10}H_{12}N_2O$, 176.1; found, 177.0 [M + H]$^+$.

(4-Methoxyphenyl)(2-phenyl-1-(phenylsulfonyl)-1*H*-imidazol-4-yl)methanone (4ab). Yield: 26.3%; mp 118−120 °C. ^{1}H NMR (500 MHz, DMSO) δ 8.37 (d, *J* = 1.0 Hz, 1 H), 8.15−8.18 (m, 2 H), 8.12 (d, *J* = 9.0 Hz, 2 H), 7.56−7.64 (m, 5 H), 7.46−7.50 (m, 3 H), 7.16 (d, *J* = 8.0 Hz, 2 H), 3.90 (s, 3 H). MS (ESI): calculated for $C_{23}H_{18}N_2O_4S$, 418.1; found, 419.1 [M + H]$^+$. HPLC2: t_R 17.72 min, purity 95.7%.

(3-Methoxyphenyl)(2-phenyl-1-(phenylsulfonyl)-1*H*-imidazol-4-yl)methanone (4ac). Yield: 31.2%; mp 136−138 °C. ^{1}H NMR (500 MHz, $CDCl_3$) δ 8.35 (s, 1 H), 7.86 (d, *J* = 8.0 Hz, 1 H),7.72 (s, 1 H), 7.60 (t, *J* = 7.5 Hz, 1 H), 7.51 (t, *J* = 7.5 Hz, 1 H), 7.35−7.42 (m, 9H), 7.14 (dd, *J* = 8.0 Hz, 2.0 Hz, 1 H), 3.88 (s, 3 H). MS (ESI): calculated for $C_{23}H_{18}N_2O_4S$, 418.1; found, 419.1 [M + H]$^+$. HPLC2: t_R 17.56 min, purity 97.4%.

(2-Phenyl-1-(phenylsulfonyl)-1*H*-imidazol-4-yl)(p-tolyl)methanone (4ah). Yield: 28.9%; mp 108−110 °C. ^{1}H NMR (500 MHz, $CDCl_3$) δ 8.00 (d, *J* = 7.5 Hz, 2 H), 7.98 (q, *J* = 8.0 Hz, 1.5 Hz, 2 H), 7.91 (d, *J* = 8.0 Hz, 1 H), 7.81 (s, 1 H), 7.44−7.48 (m, 3 H), 7.35−7.40 (m, 2 H), 7.30 (t, *J* = 8.0 Hz, 2 H), 7.20 (s, 2 H), 2.42 (s, 3 H). MS (ESI): calculated for $C_{23}H_{18}N_2O_3S$, 402.1; found, 403.1 [M + H]$^+$. HPLC2: t_R 16.06 min, purity 96.2%.

(4-Fluorophenyl)(2-phenyl-1-(phenylsulfonyl)-1*H*-imidazol-4-yl) Methanone (4af). Yield: 25.4%; mp 114−116 °C. ^{1}H NMR (500 MHz, $CDCl_3$) δ 8.10 (q, *J* = 3.5 Hz, 5.5 Hz, 2 H), 7.88 (d, *J* = 7.5 Hz, 2 H), 7.67 (t, *J* = 7.5 Hz, 1 H), 7.48−7.54 (m, 3 H), 7.38−7.41 (m, 5 H), 7.24 (t, *J* = 8.5 Hz, 2 H). MS (ESI): calculated for $C_{22}H_{15}FN_2O_3S$, 406.1; found, 429.1 [M + Na]$^+$. HPLC2: t_R 15.43 min, purity 96.1%.

(3-Fluorophenyl)(2-phenyl-1-(phenylsulfonyl)-1*H*-imidazol-4-yl) Methanone (4ag). Yield: 18.3%; mp 102−104 °C. ^{1}H NMR (500 MHz, $CDCl_3$) δ 8.14 (d, *J* = 7.5 Hz, 1 H), 7.76−7.87 (m, 3 H), 7.74 (d, *J* = 9.0 Hz, 1 H), 7.37−7.57 (m, 10 H), 7.38−7.41 (m, 5 H), 7.24 (t, *J* = 8.5 Hz, 2 H). MS (ESI): calculated for $C_{22}H_{15}FN_2O_3S$, 406.1; found, 429.1 [M + Na]$^+$. HPLC2: t_R 15.75 min, purity 96.5%.

(4-Fluorophenyl)(2-(4-methoxyphenyl)-1-(phenylsulfonyl)-1*H*-imidazol-4-yl) Methanone (4cb). Yield: 23.5%; mp 135−137 °C. ^{1}H NMR (500 MHz, $CDCl_3$) δ 8.00 (d, *J* = 5.5 Hz, 2 H), 7.74−7.76 (m, 2 H), 7.54−7.58 (m, 1 H), 7.40 (d, *J* = 7.0 Hz, 2 H), 7.28−7.30 (m, 3H), 7.14−7.16 (m, 2 H), 6.80−6.82 (m, 2 H), 3.80 (s, 3 H). MS (ESI): calculated for $C_{23}H_{17}FN_2O_4S$, 436.1; found, 459.0 [M + Na]$^+$, 434.9 [M − H]$^-$. HPLC2: t_R 16.53 min, Purity 96.1%.

(4-Fluorophenyl)(1-(phenylsulfonyl)-2-(p-tolyl)-1*H*-imidazol-4-yl) Methanone (4db). Yield: 18.6%; mp 142−144 °C. ^{1}H NMR (500 MHz, $CDCl_3$) δ 8.07 (q, *J* = 8.5 Hz, 5.5 Hz, 2 H), 7.88 (d, *J* = 7.5 Hz, 2 H), 7.64 (t, *J* = 8.0 Hz, 1 H), 7.49 (d, *J* = 8.0 Hz, 2 H), 7.38 (s, 1H), 7.30 (d, *J* = 8.0 Hz, 2 H), 7.18−7.24 (m, 4 H), 2.43 (s, 3 H). MS (ESI): calculated for $C_{23}H_{17}FN_2O_3S$, 420.1; found, 443.0 [M + Na]$^+$, 418.9 [M − H]$^-$. HPLC2: t_R 17.28 min, purity 97.3%.

(1-(Phenylsulfonyl)-2-(3,4,5-trimethoxyphenyl)-1*H*-imidazol-4-yl)(3,4,5-trimethoxyphenyl) Methanone (4ea). Yield: 21.1%; mp 135−137 °C. ^{1}H NMR (500 MHz, $CDCl_3$) δ 7.91 (d, *J* = 8.0 Hz, 2 H), 7.65 (t, *J* = 7.5 Hz, 1 H), 7.51 (t, *J* = 8.0 Hz, 2 H), 7.44 (s, 1 H), 7.34 (s, 2 H), 6.60 (s, 2 H), 3.98 (s, 3 H), 3.96 (s, 6 H), 3.91 (s, 3 H), 3.73 (s, 6 H). MS (ESI): calculated for $C_{28}H_{28}N_2O_9S$, 568.2; found, 569.2 [M + H]$^+$. HPLC1: t_R 17.86 min, purity 98.9%.

(4-Fluorophenyl)(1-(phenylsulfonyl)-2-(3,4,5-trimethoxyphenyl)-1*H*-imidazol-4-yl) Methanone (4eb). Yield: 18.8%; mp 135−137 °C.

^{1}H NMR (500 MHz, $CDCl_3$) δ 8.11 (q, J = 5.5 Hz, 3.0 Hz, 1 H), 8.00−8.03 (m, 1 H), 7.82 (d, J = 7.5 Hz, 1 H), 7.78 (s, 1 H), 7.64 (t, J = 7.0 Hz, 1 H), 7.48 (t, J = 8.0 Hz, 1 H), 7.42 (s, 1 H), 7.21−7.26 (m, 4 H), 6.62 (s, 1 H), 3.98 (s, 3 H), 3.96 (s, 6 H), 3.93 (s, 3 H). MS (ESI): calculated for $C_{25}H_{21}FN_2O_6S$, 496.1; found, 497.1 $[M + H]^+$. HPLC2: t_R 15.26 min, purity 98.5%.

(2-(4-Chlorophenyl)-1-(phenylsulfonyl)-1*H*-imidazol-4-yl)-(4-fluorophenyl) Methanone (4fb). Yield: 36.8%; mp 153−155 °C. ^{1}H NMR (500 MHz, $CDCl_3$) δ 8.06 (q, J = 5.5 Hz, 3.0 Hz, 2 H), 7.89 (d, J = 7.5 Hz, 2 H), 7.68 (t, J = 8.0 Hz, 1 H), 7.52 (t, J = 8.0 Hz, 2 H), 7.34−7.38 (m, 5H), 7.23 (t, J = 8.5 Hz, 2 H). MS (ESI): calculated for $C_{22}H_{14}ClFN_2O_3S$, 440.0; found, 463.0 $[M + Na]^+$. HPLC2: t_R 17.72 min, purity 97.4%.

(2-(4-(Dimethylamino)phenyl)-1-(phenylsulfonyl)-1*H*-imidazol-4-yl)(3,4,5-trimethoxyphenyl) Methanone (4ga). Yield: 32.2%; mp 157−159 °C. ^{1}H NMR (500 MHz, $CDCl_3$) δ 7.89 (d, J = 8.0 Hz, 2 H), 7.62 (t, J = 7.5 Hz, 1 H), 7.48 (t, J = 8.0 Hz, 2 H), 7.43 (s, 1 H), 7.32 (d, J = 8.5 Hz, 2 H), 7.30 (s, 2H), 6.62 (d, J = 9.0 Hz, 2 H), 3.97 (s, 3 H), 3.95 (s, 6 H), 3.05 (s, 6 H). MS (ESI): calculated for C27H27N3O6S, 521.2; found, 544.1 $[M + Na]^+$, 519.8 $[M - H]^-$. HPLC2: t_R 16.00 min, purity 97.9%.

(2-(4-(Dimethylamino)phenyl)-1-(phenylsulfonyl)-1*H*-imidazol-4-yl)(4-fluorophenyl) Methanone (4gb). Yield: 38.5%; mp 125−127 °C. ^{1}H NMR (500 MHz, $CDCl_3$) δ 8.04 (q, J = 5.5 Hz, 3.5 Hz, 2 H), 7.80 (d, J = 7.5 Hz, 2 H), 7.61 (t, J = 8.0 Hz, 1 H), 7.45 (t, J = 8.0 Hz, 2 H), 7.39 (s, 1 H), 7.35 (d, J = 9.0 Hz, 2 H), 7.21 (t, J = 8.5 Hz, 2 H), 6.62 (d, J = 9.0 Hz, 2 H), 3.05 (s, 6 H). MS (ESI): calculated for $C_{24}H_{20}FN_3O_3S$, 449.1; found, 472.1 $[M + Na]^+$, 447.9 $[M - H]^-$. HPLC2: t_R 16.85 min, purity 96.5%.

(2-(3,4-Dimethoxyphenyl)-1-(phenylsulfonyl)-1*H*-imidazol-4-yl)-(3,4,5-trimethoxyphenyl) Methanone (4ha). Yield: 28.6%; mp 136−138 °C. ^{1}H NMR (300 MHz, $CDCl_3$) δ 7.92 (dd, J = 8.5 Hz, 1.5 Hz, 2 H), 7.66 (t, J = 7.5 Hz, 2 H), 7.51 (t, J = 7.5 Hz, 2 H), 7.43 (s, 1 H), 7.33 (s, 2 H), 7.02 (dd, J = 8.0 Hz, 2.0 Hz, 1 H), 6.91 (d, J = 2.0 Hz, 1 H), 6.86 (d, J = 8.5 Hz, 1 H), 3.98 (s, 3 H), 3.96 (s, 9 H), 3.77 (s, 3 H). MS (ESI): calculated for $C_{27}H_{26}N_2O_8S$, 538.1; found, 561.1 $[M + Na]^+$, 536.8 $[M - H]^-$. HPLC2: t_R 14.67 min, purity 98.2%.

(2-(3,4-Dimethoxyphenyl)-1-(phenylsulfonyl)-1*H*-imidazol-4-yl)-(4-fluorophenyl) Methanone (4hb). Yield: 31.9%; mp 144−145 °C. ^{1}H NMR (300 MHz, $CDCl_3$) δ 8.09 (q, J = 5.5 Hz, 3.5 Hz, 2 H), 7.81 (d, J = 8.0 Hz, 2 H), 7.62 (t, J = 7.5 Hz, 2 H), 7.48 (t, J = 7.5 Hz, 2 H), 7.40 (s, 1 H), 7.21−7.25 (m, 2 H), 7.04 (dd, J = 8.0 Hz, 2.0 Hz, 1 H), 6.92 (d, J = 2.0 Hz, 1 H), 6.86 (d, J = 8.5 Hz, 1 H), 3.96 (s, 3 H), 3.79 (s, 6 H). MS (ESI): calculated for $C_{24}H_{19}FN_2O_5S$, 466.1; found, 489.1 $[M + Na]^+$, 464.8 $[M - H]^-$. HPLC2: t_R 15.52 min, purity 97.4%.

(1-(Phenylsulfonyl)-2-(2-(trifluoromethyl)phenyl)-1*H*-imidazol-4-yl)(3,4,5-trimethoxyphenyl) Methanone (4ia). Yield: 25.0%; mp 155−157 °C. ^{1}H NMR (500 MHz, DMSO) δ 7.91 (d, J = 8.0 Hz, 1 H), 7.84 (q, J = 7.5 Hz, 5.0 Hz, 2 H), 7.77−7.80 (m, 2 H), 7.75 (s, 2 H), 7.66 (t, J = 8.0 Hz, 2 H), 7.56 (d, J = 7.5 Hz, 1 H), 7.18 (s, 2 H), 3.87 (s, 6 H), 3.81 (s, 3 H). MS (ESI): calculated for $C_{26}H_{21}F_3N_2O_6S$, 546.1; found, 569.0 $[M + Na]^+$. HPLC2: t_R 16.16 min, purity 98.9%.

(1-(Phenylsulfonyl)-2-(2-(trifluoromethyl)phenyl)-1*H*-imidazol-4-yl)(4-fluorophenyl) Methanone (4ib). Yield: 25.0%; mp 151−153 °C. ^{1}H NMR (500 MHz, $CDCl_3$) δ 8.03 (q, J = 5.5 Hz, 3.0 Hz, 2 H), 7.90 (d, J = 8.0 Hz, 2 H), 7.80 (d, J = 8.0 Hz, 1 H), 7.69 (q, J = 7.0 Hz, 6.5 Hz, 2 H), 7.61 (t, J = 8.0 Hz, 1 H), 7.52 (t, J = 8.0 Hz, 2 H), 7.34−7.36 (m, 2 H), 7.23 (t, J = 8.5 Hz, 2 H). MS (ESI): calculated for $C_{23}H_{14}F_4N_2O_3S$, 474.1; found, 497.0 $[M + Na]^+$. HPLC2: t_R 16.80 min, purity 98.2%.

(2-(4-(Benzyloxy)phenyl)-1-(phenylsulfonyl)-1*H*-imidazol-4-yl)-(4-fluorophenyl) Methanone (4jb). Yield: 22.3.0%; mp 149−151 °C. ^{1}H NMR (500 MHz, $CDCl_3$) δ 8.09 (q, J = 5.5 Hz, 3.5 Hz, 2 H), 7.82 (d, J = 7.5 Hz, 2 H), 7.63 (t, 7.5 Hz, 1 H), 7.36−7.50 (m, 10 H), 7.25 (t, J = 8.5 Hz, 2 H), 6.98 (d, J = 8.0 Hz, 2 H), 5.17 (s, 2 H). MS (ESI): calculated for $C_{29}H_{21}FN_2O_4S$, 512.1; found, 535.0 $[M + Na]^+$. HPLC2: t_R 18.35 min, purity 95.1%.

(1-(Phenylsulfonyl)-2-(4-(trifluoromethyl)phenyl)-1*H*-imidazol-4-yl)(3,4,5-trimethoxyphenyl) Methanone (4la). Yield: 36.7%. ^{1}H NMR ($CDCl_3$, 500 MHz) δ 8.06 (d, J = 7.5 Hz, 2 H), 7.78 (t, J = 8.0 Hz, 1 H), 7.72 (d, J = 8.0 Hz, 2 H), 7.62 (d, J = 8.0 Hz, 2 H),, 7.59 (d, J = 8.0 Hz, 2 H), 7.50 (s, 1 H), 7.37 (s, 2 H), 4.04 (s, 3 H), 4.02 (s, 6 H). MS (ESI) calculated for $C_{26}H_{21}F_3N_2O_6S$, 546.1; found, 547.1 $[M + H]^+$.

(2-Phenyl-1*H*-imidazol-4-yl)(3,4,5-trimethoxyphenyl) Methanone (5aa). Yield: 10.1%; mp 227−229 °C. ^{1}H NMR (500 MHz, $CDCl_3$) δ 8.0−8.03 (m, 2 H), 7.83 (s, 1 H), 7.34−7.38 (m, 3 H), 7.21 (s, 2 H), 3.90 (s, 3 H), 3.84 (s, 6 H). MS (ESI): calculated for $C_{19}H_{18}N_2O$, 338.1; found 337.1 $[M - H]^-$. HPLC2: t_R14.19 min, purity 96.3%.

(4-Methoxyphenyl)(2-phenyl-1*H*-imidazol-4-yl) Methanone (5ab). Yield: 16.6%; mp 179−181 °C. ^{1}H NMR (500 MHz, $CDCl_3$) δ 11.1 (br, 1 H), 8.07−8.10 (m, 2 H), 8.04 (d, J = 8.5 Hz, 2 H), 7.84 (d, J = 1.0 Hz, 1 H), 7.49−7.51 (m, 3 H), 7.07 (d, J = 9.0 Hz, 2 H), 3.95 (s, 3 H). MS (ESI): calculated for $C_{17}H_{14}N_2O_2$, 278.1; found, 279.0 $[M + H]^+$. HPLC1: t_R 15.14 min, purity >99%.

(3-Methoxyphenyl)(2-phenyl-1*H*-imidazol-4-yl) Methanone (5ac). Yield: 22.5%; mp 160−162 °C. ^{1}H NMR (500 MHz, $CDCl_3$) δ 11.2 (br, 1 H), 8.10−8.12 (m, 2 H), 7.87 (d, J = 1.0 Hz, 1 H), 7.61 (d, J = 7.5 Hz, 1 H), 7.48−7.52 (m, 5 H), 7.21 (dd, J = 2.5 Hz, 8.5 Hz, 1 H), 3.91 (s, 3 H). MS (ESI): calculated for $C_{17}H_{14}N_2O_2$, 278.1; found, 279.0 $[M + H]^+$. HPLC2: t_R 15.07 min, purity >99%.

(3,5-Dimethoxyphenyl)(2-phenyl-1*H*-imidazol-4-yl) Methanone (5ad). Yield: 26.2%; mp 168−170 °C. ^{1}H NMR (500 MHz, $CDCl_3$) δ 8.04−8.06 (m, 2 H), 7.88 (s, 1 H), 7.50−7.52 (m, 3 H), 7.15 (d, J = 2.0 Hz, 2 H), 6.75 (t, J = 1.0 Hz, 1 H), 3.89 (s, 6 H). MS (ESI): calculated for $C_{18}H_{16}N_2O_3$, 308.1; found, 331.1 $[M + Na]^+$, 306.9 $[M - H]^-$. HPLC2: t_R 15.59 min, purity >99%.

(3,4-Dimethoxyphenyl)(2-phenyl-1*H*-imidazol-4-yl) Methanone (5ae). Yield: 18.6%; mp 162−164 °C. ^{1}H NMR (500 MHz, $CDCl_3$) δ 10.9 (br, 1 H), 8.05 (dd, J = 1.5 Hz, 8.0 Hz, 2 H), 7.86 (d, J = 1.5 Hz, 1 H), 7.74 (dd, J = 2.0 Hz, 8.5 Hz, 1 H), 7.56 (d, J = 2.0 Hz, 1 H), 7.50−7.52 (m, 3 H), 7.04 (d, J = 8.5 Hz, 1 H), 4.03 (s, 3 H), 3.99 (s, 3 H). MS (ESI): calculated for $C_{18}H_{16}N_2O_3$, 308.1; found, 331.1 $[M + Na]^+$, 306.9 $[M - H]^-$. HPLC2: t_R 13.54 min, purity >99%.

(4-Fluorophenyl)(2-phenyl-1*H*-imidazol-4-yl) Methanone (5af). Yield: 30.2%; mp 231−233 °C. ^{1}H NMR (500 MHz, $CDCl_3$) δ 10.6 (br, 1 H), 8.02−8.05 (m, 4 H), 7.81 (d, J = 1.0 Hz, 1 H), 7.51−7.54 (m, 3 H), 7.27 (t, J = 8.5 Hz, 2 H). MS (ESI): calculated for $C_{16}H_{11}FN_2O$, 266.1; found, 267.0 $[M + H]^+$, 264.8 $[M - H]^-$. HPLC1: t_R 15.37 min, purity 98.9%.

(3-Fluorophenyl)(2-phenyl-1*H*-imidazol-4-yl) Methanone (5ag). Yield: 23.4%; mp 212−214 °C. ^{1}H NMR (500 MHz, $CDCl_3$) δ 8.05 (dd, J = 1.5 Hz, 7.5 Hz, 2 H), 7.86 (s, 1 H), 7.84 (d, J = 7.0 Hz, 1 H), 7.74 (d, J = 8.5 Hz, 1 H), 7.52−7.58 (m, 4 H), 7.37 (dt, J = 2.0 Hz, 6.0 Hz, 1 H). MS (ESI): calculated for $C_{16}H_{11}FN_2O$, 266.1; found, 267.0 $[M + H]^+$, 264.8 $[M - H]^-$. HPLC1: t_R 15.29 min, purity >99%.

(2-Phenyl-1*H*-imidazol-4-yl)(*p*-tolyl) Methanone (5ah). Yield: 15.6%; mp 225−227 °C. ^{1}H NMR (500 MHz, $CDCl_3$) δ 11.1 (br, 1 H), 8.08 (d, J = 7.5 Hz, 2 H), 7.93 (d, J = 9.0 Hz, 2 H), 7.84 (s, 1 H), 7.48−7.52 (m, 3 H), 7.38 (d, J = 10.0 Hz, 2 H), 2.50 (s, 3 H). MS (ESI): calculated for $C_{17}H_{14}N_2O$, 262.1; found, 263.0 $[M + H]^+$, 260.8 $[M - H]^-$. HPLC2: t_R 15.86 min, purity 98.7%.

(2-Phenyl-1*H*-imidazol-4-yl)(*m*-tolyl) Methanone (5ai). Yield: 20.5%; mp 168−169 °C. ^{1}H NMR (500 MHz, $CDCl_3$) δ 11.0 (br, 1 H), 8.09−8.11 (m, 2 H), 7.84 (d, J = 1.5 Hz, 1 H), 7.81−7.82 (m, 2 H), 7.47−7.52 (m, 5 H), 2.50 (s, 3 H). MS (ESI): calculated for $C_{17}H_{14}N_2O$, 262.1; found, 285.0 $[M + Na]^+$, 260.8 $[M - H]^-$. HPLC2: t_R 15.89 min, purity >99%.

(2-(4-Fluorophenyl)-1*H*-imidazol-4-yl)(3,4,5-trimethoxyphenyl) Methanone (5ba). Yield: 12.2%; mp 176−178 °C. ^{1}H NMR (500 MHz, $CDCl_3$) δ 10.72 (br, 1 H), 8.02 (q, J = 5.0 Hz, 2 H), 7.84 (s, 1 H), 7.19 (t, J = 10.0 Hz, 2 H), 4.00 (s, 6 H), 3.97 (s, 3 H). MS (ESI): calculated for $C_{19}H_{17}FN_2O_4$, 356.1; found, 379.1 $[M + Na]^+$, 354.9 $[M - H]^-$. HPLC1: t_R 17.23 min, purity >99%

(2-(4-Methoxyphenyl)-1*H*-imidazol-4-yl)(3,4,5-trimethoxyphenyl) Methanone (5ca). Yield: 10.2%; mp 220−222 °C. ^{1}H NMR (300 MHz, CDCl$_3$) δ 10.24 (br, 1 H), 7.93 (d, J = 14.5 Hz, 2 H), 7.81 (s, 1 H), 7.24 (s, 2 H), 7.03 (d, J = 14.5 Hz, 2 H), 3.97 (s, 3 H), 3.95 (s, 6 H), 3.90 (s, 3 H). MS (ESI): calculated for $C_{20}H_{20}N_2O_5$, 368.1; found, 391.0 [M + Na]$^+$, 367.0 [M − H]$^-$. HPLC2: t_R 14.46 min, purity 98.4%.

(4-Fluorophenyl)(2-(4-methoxyphenyl)-1*H*-imidazol-4-yl) Methanone (5cb). Yield: 15.2%; mp 245−247 °C. ^{1}H NMR (500 MHz, CDCl$_3$) δ 10.20 (br, 1 H), 7.93−7.96 (m, 2 H), 7.85 (d, J = 5.0 Hz, 2 H), 7.68 (s, 1 H), 7.15−7.17 (m, 2 H), 6.95 (d, J = 6.0 Hz, 2 H), 3.82 (s, 3 H). MS (ESI): calculated for $C_{17}H_{13}FN_2O_2$, 296.1; found, 319.1 [M + Na]$^+$, 294.9 [M − H]$^-$. HPLC2: t_R 15.40 min, purity 98.8%.

(2-(*p*-Tolyl)-1*H*-imidazol-4-yl)(3,4,5-trimethoxyphenyl) Methanone (5da). Yield: 48.5%; mp 201−203 °C. ^{1}H NMR (500 MHz, CDCl$_3$) δ 10.40 (br, 1 H), 7.88 (d, J = 8.0 Hz, 2 H), 7.82 (s, 1 H), 7.31 (d, J = 8.0 Hz, 2 H), 7.24 (s, 2 H), 3.96 (s, 3 H), 3.94 (s, 6 H), 2.43 (s, 3 H). MS (ESI): calculated for $C_{20}H_{20}N_2O_4$, 352.1; found, 375.2 [M + Na]$^+$. HPLC2: t_R 15.45 min, purity 97.4%.

(4-Fluorophenyl)(2-(*p*-tolyl)-1*H*-imidazol-4-yl) Methanone (5db). Yield: 56.3%; mp 229−231 °C. ^{1}H NMR (500 MHz, CDCl$_3$) δ 10.50 (br, 1 H), 7.99−8.02 (m, 2 H), 7.88 (d, J = 8.0 Hz, 2 H), 7.60 (d, J = 1.0 Hz, 1 H), 7.30 (d, J = 8.0 Hz, 2 H), 7.23 (t, J = 9.0 Hz, 2 H), 2.43 (s, 3 H). MS (ESI): calculated for $C_{17}H_{13}FN_2O$, 280.1; found, 281.0 [M + H]$^+$, 278.9 [M − H]$^-$. HPLC2: t_R 16.31 min, purity > 99%.

(3,4,5-Trimethoxyphenyl)(2-(3,4,5-trimethoxyphenyl)-1*H*-imidazol-4-yl) Methanone (5ea). Yield: 86.8%; mp 196−198 °C. ^{1}H NMR (500 MHz, DMSO) δ 13.3 (br, 0.47 H), 13.50 (br, 0.52 H), 8.19 (s, 0.49 H), 7.90 (s, 1 H), 7.83 (s, 0.5 H), 7.59 (s, 1 H), 7.40 (s, 1 H), 7.18 (s, 1 H), 3.89 (s, 6 H), 3.86 (s, 6 H), 3.77 (s, 3 H), 3.72 (s, 3 H). MS (ESI): calculated for $C_{22}H_{24}N_2O_7$, 428.2; found, 451.1 [M + Na]$^+$, 426.9 [M − H]$^-$. HPLC2: t_R 14.49 min, purity > 99%.

(4-Fluorophenyl)(2-(3,4,5-trimethoxyphenyl)-1*H*-imidazol-4-yl) Methanone (5eb). Yield: 90.2%; mp 153−155 °C. ^{1}H NMR (500 MHz, CDCl$_3$) δ 10.42 (br, 1 H), 8.00 (q, J = 5.5 Hz, 3.0 Hz, 2 H), 7.76 (s, 1H), 7.23 (t, J = 8.5 Hz, 2 H), 7.19 (s, 2 H), 3.94 (s, 3 H), 3.92 (s, 3 H). MS (ESI): calculated for $C_{19}H_{17}FN_2O_4$, 356.1; found, 379.0 [M + Na]$^+$, 354.9 [M − H]$^-$. HPLC2: t_R 15.31 min, purity > 99%.

(2-(4-Chlorophenyl)-1*H*-imidazol-4-yl)(3,4,5-trimethoxyphenyl) Methanone (5fa). Yield: 36.9%; mp 193−195 °C. ^{1}H NMR (500 MHz, CDCl$_3$) δ 10.75 (br, 1 H), 7.96 (d, J = 8.5 Hz, 2 H), 7.83 (s, 1 H), 7.47 (d, J = 9.0 Hz, 2 H), 7.23 (s, 2 H), 3.97 (s, 3 H), 3.94 (s, 6 H), 2.43 (s, 3 H). MS (ESI): calculated for $C_{19}H_{17}ClN_2O_4$, 372.1; found, 395.1 [M + Na]$^+$, 370.9 [M − H]$^-$. HPLC2: t_R 16.36 min, purity > 99%.

(2-(4-Chlorophenyl)-1*H*-imidazol-4-yl)(4-fluorophenyl) Methanone (5fb). Yield: 83.7%; mp 232−234 °C. ^{1}H NMR (500 MHz, CDCl$_3$) δ 10.78 (br, 1 H), 8.00 (q, J = 5.5 Hz, 3.0 Hz, 2 H), 7.96 (d, J = 9.0 Hz, 2 H), 7.78 (s, 1 H), 7.47 (d, J = 8.0 Hz, 2 H), 7.24 (t, J = 8.5 Hz, 2 H). MS (ESI): calculated for $C_{16}H_{10}ClFN_2O$, 300.1; found, 323.0 [M + Na]$^+$, 298.8 [M − H]$^-$. HPLC2: t_R 17.08 min, purity > 99%.

(2-(4-(Dimethylamino)phenyl)-1*H*-imidazol-4-yl)(3,4,5-trimethoxyphenyl) Methanone (5ga). Yield: 91.2%; mp 195−197 °C. ^{1}H NMR (500 MHz, CDCl$_3$) δ 10.39 (br, 1 H), 7.87 (d, J = 8.5 Hz, 2 H), 7.80 (s, 1 H), 7.23 (s, 2 H), 6.75(d, J = 9.0 Hz, 2 H), 3.95 (s, 3 H), 3.94 (s, 6 H), 3.05 (s, 6 H). MS (ESI): calculated for $C_{21}H_{23}N_3O_4$, 381.2; found, 404.2 [M + Na]$^+$, 380.0 [M − H]$^-$. HPLC2: t_R 15.20 min, purity 95.8%.

(2-(4-(Dimethylamino)phenyl)-1*H*-imidazol-4-yl)(4-fluorophenyl) Methanone (5gb). Yield: 86.7%; mp 278−280 °C. ^{1}H NMR (500 MHz, CDCl$_3$) δ 10.21 (br, 1 H), 7.98 (q, J = 5.0 Hz, 3.5 Hz, 2 H), 7.84 (d, J = 8.5 Hz, 2 H), 7.72 (s, 1 H), 7.20 (t, J = 8.5 Hz, 2 H), 6.76 (t, J = 9.0 Hz, 2 H), 3.06 (s, 6 H). MS (ESI): calculated for $C_{18}H_{16}FN_3O$, 309.1; found, 332.1 [M + Na]$^+$, 307.9 [M − H]$^-$. HPLC2: t_R 16.06 min, purity 95.6%.

(2-(3,4-Dimethoxyphenyl)-1*H*-imidazol-4-yl)(3,4,5-trimethoxyphenyl) Methanone (5ha). Yield: 85.0%; mp 100−102 °C. ^{1}H NMR (500 MHz, CDCl$_3$) δ 10.19 (br, 1 H), 7.81 (s, 1 H), 7.58 (d, J = 1.5 Hz, 1 H), 7.48 (d, J = 8.0 Hz, 1 H), 7.25 (s, 2 H), 6.97 (d, J = 8.5 Hz, 1 H), 4.00 (s, 3 H), 3.96 (s, 6 H), 3.95 (s, 6 H). MS (ESI): calculated for $C_{21}H_{22}N_2O_6$, 398.2; found, 399.1 [M + H]$^+$, 397.0 [M − H]$^-$. HPLC2: t_R 13.73 min, purity > 99%.

(2-(3,4-Dimethoxyphenyl)-1*H*-imidazol-4-yl)(4-fluorophenyl) Methanone (5hb). Yield: 78.3%; mp 174−176 °C. ^{1}H NMR (500 MHz, CDCl$_3$) δ 8.02 (t, J = 9.0 Hz, 2 H), 7.75 (s, 1 H), 7.57 (s, 1 H), 7.48 (d, J = 8.5 Hz, 1 H), 7.23 (t, J = 8.5 Hz, 2 H), 6.95 (d, J = 8.5 Hz, 1 H), 3.99 (s, 3 H), 3.96 (s, 3 H). MS (ESI): calculated for $C_{18}H_{15}FN_2O_3$, 326.1; found, 349.0 [M + Na]$^+$, 324.9 [M − H]$^-$. HPLC2: t_R 14.65 min, purity > 99%.

(2-(2-(Trifluoromethyl)phenyl)-1*H*-imidazol-4-yl)(3,4,5-trimethoxyphenyl) Methanone (5ia). Yield: 83.8%; mp 75−77 °C. ^{1}H NMR (500 MHz, CDCl$_3$) δ 10.37 (br, 1 H), 8.00−8.02 (m, 1 H), 7.87 (s, 1 H), 7.82−7.85 (m, 1 H), 7.69−7.74 (m, 1 H), 7.62−7.66 (m, 1 H), 7.25 (s, 2 H), 3.99 (s, 3 H), 3.98 (s, 6 H). MS (ESI): calculated for $C_{20}H_{17}F_3N_2O_4$, 406.1; found, 429.1 [M + Na]$^+$, 405.0 [M − H]$^-$. HPLC2: t_R 13.98 min, purity > 99%.

(4-Fluorophenyl)(2-(2-(trifluoromethyl)phenyl)-1*H*-imidazol-4-yl) Methanone (5ib). Yield: 91.1%; mp 152−154 °C. ^{1}H NMR (500 MHz, CDCl$_3$) δ 8.12−8.14 (m, 2 H), 7.97 (d, J = 7.5 Hz, 1 H), 7.82−7.85 (m, 2 H), 7.69 (t, J = 7.5 Hz, 1 H), 7.61 (t, J = 8.0 Hz, 1 H), 7.22 (t, J = 9.0 Hz, 2 H). MS (ESI): calculated for $C_{17}H_{10}F_4N_2O$, 334.1; found, 357.1 [M + Na]$^+$, 332.9 [M − H]$^-$. HPLC2: t_R 15.10 min, purity > 99%.

(2-(4-(Benzyloxy)phenyl)-1*H*-imidazol-4-yl)(3,4,5-trimethoxyphenyl) Methanone (5ja). Yield: 16.5%; mp 191−193 °C. ^{1}H NMR (500 MHz, CDCl$_3$) δ 10.22 (br, 1 H), 7.93 (d, J = 9.0 Hz, 2 H), 7.81 (s, 1 H), 7.37−7.47 (m, 5 H), 7.24 (s, 2 H), 7.11 (d, J = 8.5 Hz, 2 H), 5.16 (s, 2 H), 3.97 (s, 3 H), 3.95 (s, 6 H). MS (ESI): calculated for $C_{26}H_{24}N_2O_5$, 444.2; found, 467.1 [M + Na]$^+$, 442.9 [M − H]$^-$. HPLC2: t_R 17.36 min, purity 95.5%.

(2-(4-(Benzyloxy)phenyl)-1*H*-imidazol-4-yl)(4-fluorophenyl) Methanone (5jb). Yield: 84.7%; mp 212−214 °C. ^{1}H NMR (300 MHz, CDCl$_3$) δ 10.28 (br, 1 H), 799−8.04 (m, 2 H), 7.92−7.95 (m, 2 H), 7.76 (d, J = 1.5 Hz, 1 H), 7.38−7.48 (m, 5 H), 7.20−7.25 (m, 2 H), 7.09−7.12 (m, 2 H), 5.16 (s, 2 H). MS (ESI): calculated for $C_{23}H_{17}FN_2O_2$, 372.1; found, 395.1 [M + Na]$^+$. HPLC2: t_R 17.97 min, purity 97.8%.

(2-(4-Hydroxyphenyl)-1*H*-imidazol-4-yl)(3,4,5-trimethoxyphenyl) Methanone (5ka). Yield: 72.3%. mp 191−193 °C. ^{1}H NMR (500 MHz, CD$_3$OD) δ 8.31 (s, 1 H), 7.90 (d, J = 8.5 Hz, 2 H), 7.31 (s, 2 H), 7.05 (s, 2 H), 3.95 (s, 6 H), 3.88 (s, 3 H). MS (ESI): calculated for $C_{19}H_{18}N_2O_5$, 354.1; found, 355.1 [M + H]$^+$, 352.9 [M − H]$^-$. HPLC2: t_R 12.25 min, purity 98.7%.

(2-(4-(Hydroxyphenyl)-1*H*-imidazol-4-yl)(4-fluorophenyl) Methanone (5kb). Yield: 89.0%; mp 276−278 °C. ^{1}H NMR (500 MHz, CDCl$_3$) δ 8.31 (s, 1 H), 8.13 (q, J = 5.5 Hz, 3.0 Hz, 2 H), 7.93 (d, J = 8.5 Hz, 2 H), 7.38 (t, J = 8.5 Hz, 2 H), 7.07 (d, J = 8.5 Hz, 2 H). MS (ESI): calculated for $C_{16}H_{11}FN_2O_2$, 282.1; found, 283.0 [M + H]$^+$, 280.9 [M − H]$^-$. HPLC2: t_R 13.46 min, purity 97.7%.

(2-(4-(Trifluoromethyl)phenyl)-1*H*-imidazol-4-yl)(3,4,5-trimethoxyphenyl) Methanone (5la). Yield: 85.3%; mp 195−196 °C. ^{1}H NMR (CDCl$_3$, 500 MHz) δ 8.22 (d, J = 8.5 Hz, 2 H), 7.96 (s, 1 H), 7.83 (d, J = 8.5 Hz, 2 H), 7.34 (s, 2 H), 4.04 (s, 3 H), 4.00 (s, 6 H). MS (ESI) calcd for $C_{20}H_{17}F_3N_2O_4$, 406.1; found, 407.1 [M + H]$^+$. HPLC2: t_R 18.00 min, purity > 99%.

(2-Phenyl-1*H*-imidazol-1-yl)(3,4,5-trimethoxyphenyl) Methanone (5aaa). Yield: 39.8%; mp 113−115 °C. ^{1}H NMR (500 MHz, CDCl$_3$) δ 7.53 (q, J = 5.0 Hz, 3.0 Hz, 2 H), 7.41 (d, J = 1.0 Hz, 1 H), 7.33−7.35 (m, 3 H), 7.23 (d, J = 1.0 Hz, 1 H), 7.03 (s, 2 H), 3.93 (s, 3 H), 3.85 (s, 6 H). MS (ESI): calculated for $C_{19}H_{18}N_2O_4$, 338.1; found, 339.1 [M + H]$^+$. HPLC2: t_R 13.8 min, purity 95.6%.

(4-Methoxyphenyl)(2-phenyl-1*H*-imidazol-1-yl) Methanone (5aba). Yield: 56.3%; mp 68−70 °C. ^{1}H NMR (500 MHz, CDCl$_3$) δ 7.78 (d, J = 9.0 Hz, 2 H), 7.54−7.56 (m, 2 H), 7.32−7.34 (m, 4 H), 7.21 (d, $J = 1.0$ Hz, 1 H), 6.93 (d, $J = 8.5$ Hz, 2 H), 3.90 (s, 3 H). MS (ESI): calculated for $C_{17}H_{14}N_2O_2$, 278.1; found, 301.0 $[M + Na]^+$, 276.8 $[M - H]^-$. HPLC2: t_R 14.72 min, purity 95.7%.

(4-Fluorophenyl)(2-(*p*-tolyl)-1*H*-imidazol-4-yl) Methanone HCl Salt (5db-HCl). Yield: 95%; mp 115−117 °C. ^{1}H NMR (500 MHz, DMSO) δ 8.20−8.23 (m, 2 H), 8.18 (s, 1 H), 8.04 (d, $J = 6.5$ Hz, 2 H), 7.42 (t, $J = 8.0$ Hz, 2 H), 7.37 (d, $J = 7.0$ Hz, 2 H), 2.38 (s, 3 H). MS (ESI): calculated for $C_{17}H_{14}FClN_2O$, 316.1; found, 281.0 $[M - HCl + H]^+$. HPLC2: t_R 17.16 min, purity >99%.

(3,4,5-Trihydroxyphenyl)(2-(3,4,5-trihydroxyphenyl)-1*H*-imidazol-4-yl) Methanone (6ea). Yield: 66.1%; mp 294−296 °C. ^{1}H NMR (500 MHz, CD_3OD) δ 8.07 (s, 1 H), 7.07 (s, 2 H), 7.02 (s, 2 H). MS (ESI): calculated for $C_{16}H_{12}N_2O_7$, 344.1; found, 345.0 $[M + H]^+$, 342.9 $[M - H]^-$. HPLC2: t_R 3.62 min, purity 97.9%.

(2-(4-Chlorophenyl)-1*H*-imidazol-4-yl)(3,4,5-trihydroxyphenyl) Methanone (6fa). Yield: 79.3%; mp > 300 °C. ^{1}H NMR (500 MHz, CD_3OD) δ 8.02 (d, $J = 8.5$ Hz, 2 H), 7.77 (s, 1 H), 7.54 (d, $J = 8.5$ Hz, 2 H), 7.14 (s, 2 H). MS (ESI): calculated for $C_{16}H_{11}ClN_2O_4$, 330.0; found, 331.1 $[M + Na]^+$, 328.9 $[M - H]^-$. HPLC2: t_R 11.9 min, purity 95.6%.

(2-(3,4-Dihydroxyphenyl)-1*H*-imidazol-4-yl)(3,4,5-trihydroxyphenyl) Methanone (6ha). Yield: 62.2%; mp > 300 °C. ^{1}H NMR (500 MHz, CD_3OD) δ 8.11 (s, 1 H), 7.46 (d, $J = 2.0$ Hz, 1 H), 7.42 (dd, $J = 8.5$ Hz, 2.0 Hz, 1 H), 7.10 (s, 2 H), 7.02 (d, $J = 8.5$ Hz, 1 H). MS (ESI): calculated for $C_{16}H_{12}N_2O_6$, 328.1; found, 329.0 $[M + H]^+$, 326.9 $[M - H]^-$. HPLC2: t_R 3.64 min, purity 97.9%.

Determination of Aqueous Solubility. The aqueous solubility of selected compounds was estimated using a miniaturized shake-flask method.[32] Approximately 1 mg of each compound was suspended in either 1 mL water or pH 7.0 buffer in a glass vial and shaken at 450 rpm for 24 h at room temperature. The resulting mixture was centrifuged at 21000*g* for 10 min, and the concentration in the supernatant was measured by Acquity LC-MS/MS consisting of triple quadrupole mass spectrometer (Waters, Milford, MA) that was operated in positive ion mode with electrospray ionization. Chromatographic separation of the analytes was performed using a C6-phenyl column (50 mm × 2.1 mm i.d, 3.5 μM) (Phenomenex, Torrance, CA) with guard column, applying isocratic elution with water (10%) and acetonitrile (90%). The flow rate was set to 0.5 mL/min.

Biology

Cell Culture and Cytotoxicity Assay. We examined the antiproliferative activity of the ABI compounds in three melanoma cell lines (A375 and WM-164, human melanoma cell line; B16−F1, mouse melanoma cell line) and four human prostate cancer cell lines (LNCaP, DU 145, PC-3, and PPC-1). All these cell lines were purchased from ATCC (American Type Culture Collection, Manassas, VA) except the PPC-1 cell line, which was kindly provided by Dr. Mitchell Steiner at the University of Tennessee Health Science Center. MDA-MB-435 and MDA-MB-435/LCCMDR1 cells were kindly provided by Dr. Robert Clarke at Georgetown University School of Medicine, Washington, DC. Melanoma cells were cultured in DMEM (Cellgro Mediatech, Inc., Herndon, VA), and prostate cancer cells were cultured in RPMI 1640 (Cellgro Mediatech, Inc., Herndon, VA) supplemented with 10% FBS (Cellgro Mediatech). Cultures were maintained at 37 °C in a humidified atmosphere containing 5% CO_2. Then 1000−5000 cells were plated into each well of 96-well plates depending on growth rate and exposed to different concentrations of a test compound for 48 h (fast growing melanoma cells) or 96 h (slow growing prostate cancer cells) in three−five replicates. Cell numbers at the end of the drug treatment were measured by the sulforhodamine B (SRB) assay. Briefly, the cells were fixed with 10% trichloroacetic acid and stained with 0.4% SRB, and the absorbances at 540 nm were measured using a plate reader (DYNEX Technologies, Chantilly, VA). Percentages of cell survival versus drug concentrations were plotted, and the IC_{50} (concentration that inhibited cell growth by 50% of untreated control) values were obtained by nonlinear regression analysis using GraphPad Prism (GraphPad Software, San Diego, CA).

Animals. Female C57/BL mice, age 4−6 weeks, were purchased from Harlan Laboratories (Harlan Laboratories Inc., Indianapolis, IN). Our animal housing met the Association for Assessment and Accreditation and Laboratory Animal Care specifications. All of the procedures were conducted in accordance with guidelines of our Institutional Animal Care and Use Committee.

In Vivo Evaluation of Efficacy. Mouse melanoma B16−F1 cells were prepared in FBS-free DMEM medium (Cellgro Mediatech) at a concentration of 5×10^6 viable cells/mL. The cell suspension (100 μL) was injected subcutaneously in the right dorsal flank of each mouse. When tumor size reached about 100−150 mm^3, about 7 days after cell inoculation, all mice bearing tumors were divided into control and treatment groups based on tumor size ($n = 5$ per group). Each group had similar average tumor size. Mice in control groups (negative control) were injected intraperitoneally with 50 μL of vehicle solution only or DTIC at 60 mg/kg (positive control) once daily.[24] Tumor volume was measured every 2 days with a Traceable electronic digital caliper (Fisher Scientific, Inc., Pittsburgh, PA) and calculated using the formula $a \times b^2 \times 0.5$, where a and b represented the larger and smaller diameters, respectively.[33] Tumor volume was expressed in cubic millimeters. Data were expressed as mean ± SE for each group and plotted as a function of time. Percentage tumor reduction at the conclusion of the experiment (14 days after starting treatment) was calculated with the formula $100 - 100 \times [(T - T_0)/(C - C_0)]$, where T represents mean tumor volume of a treated group on a specific day, T_0 represents mean tumor volume of the same group on the first day of treatment, C represents mean tumor volume of a control on a specific day, and C_0 represents mean tumor volume of the same group on the first day of treatment. Animal activity and average body weight of each group were monitored during the entire experiment period to assess compound toxicity. At the end of treatment, all mice were euthanized by CO_2 followed by cervical dislocation, and tumors were harvested for further studies.

In Vitro Microtubule Polymerization Assay. Bovine brain tubulin (0.4 mg) (Cytoskeleton, Denver, CO) was mixed with 10 μM of the test compound and incubated in 110 μL of general tubulin buffer (80 mM PIPES, 2.0 mM $MgCl_2$, 0.5 mM EGTA, and 1 mM GTP) at pH 6.9. The absorbance at 340 nm was monitored every 1 min for 15 min by the SYNERGY 4 microplate reader (Bio-Tek Instruments, Winooski, VT). The spectrophotometer was set at 37 °C for tubulin polymerization.

Competitive Colchicine Binding Assay. Each test compound was prepared at 20× concentration in G-PEM buffer (Cytoskeleton Inc., Denver, CO) followed by pipetting 10 μL of test compound into the 96-well plates. Ten μL of tritiated labeled colchicine (Perkin-Elmer, Waltham, MA) was added to each testing well. Subsequently, 180 μL of bead/tubulin (GE Healthcare Bio-Sciences Corp., Piscataway, NJ) suspension was added into each well. The plate was incubated for 45 min at 37 °C before it was read by a Topcount NXT plate reader (Perkin-Elmer, Waltham, MA). We included nonradiolabeled "cold" colchicine as a positive control and paclitaxel as a negative control because paclitaxel binds to a different site in tubulin and does not compete for the colchicine site binding. Data were processed using GraphPad Prism software.

Molecular Modeling. All molecular modeling studies were performed with Schrodinger Molecular Modeling Suite 2009 (Schrodinger LLC, New York, NY), running on a Dell Linux workstation. Because the size of ABI compounds is much closer to that of ABT-751, rather than DAMA-colcochine, we selected tubulin complex with ABT-751 (PDB code: 3KHC) as our modeling system. ABIs were built and prepared using the Ligprep module, and they were docked into the ABT-751 site using the

Glide module in Schrodinger Suite. The best docking complexes were subject to restricted molecular dynamics to release any strains using Macromodel module with OPLS-2005 force field. The ligand and its surrounding residues within 15 Å were allowed to move freely, while residues outside the 15 Å radius were kept rigid.

Acknowledgment. The project was supported by grant no. 1R15CA125623-01A2 from NIH/NCI. Its contents are solely the responsibility of the authors and do not necessarily represent the official views of the NIH. Additional support comes from the Van Vleet Endowed Professorship (DDM), Division of Pharmaceutics, The Ohio State University, and GTx, Inc. Zhao Wang acknowledges the support from the Alma & Hal Reagan Fellowship. We thank Drs. Vivian S. Loveless and Christina Barrett for their help in the tubulin colchicine site binding assay and Dr. Ryan Yates for providing access to an HPLC instrument. We also thank Dr. David Armbruster, University of Tennessee Health Science Center library, for his editorial assistance.

Supporting Information Available: Dose–response curves in Pgp-mediated multidrug resistant and their parental sensitive melanoma cell lines for compounds **5cb**, **4cb**, and **4fb**; competitive binding at the colchicine site in tubulin for compound **5cb**; analytical and spectroscopic data for all final compounds. This material is available free of charge via the Internet at http://pubs.acs.org.

References

(1) Chen, J.; Wang, Z.; Lu, Y.; Dalton, J. T.; Miller, D. D.; Li, W. Synthesis and antiproliferative activity of imidazole and imidazoline analogs for melanoma. *Bioorg. Med. Chem. Lett.* **2008**, *18*, 3183–3187.
(2) Lu, Y.; Li, C. M.; Wang, Z.; Ross, C. R., II; Chen, J.; Dalton, J. T.; Li, W.; Miller, D. D. Discovery of 4-substituted methoxybenzoyl-aryl-thiazole as novel anticancer agents: synthesis, biological evaluation, and structure–activity relationships. *J. Med. Chem.* **2009**, *52*, 1701–1711.
(3) Li, F.; Lu, Y.; Li, W.; Miller, D. D.; Mahato, R. I. Synthesis, formulation and in vitro evaluation of a novel microtubule destabilizer, SMART-100. *J. Controlled Release* **2010**, *143*, 151–158.
(4) Amir, E.; Rozen, S. Easy access to the family of thiazole *N*-oxides using HOF·CH3CN. *Chem. Commun.* (*Cambridge*) **2006**, 2262–2264.
(5) Williams, D. A.; Lemke, T. L. Foye's Principles of Medicinal Chemistry, 5th ed.; Lippincott Williams & Wilkins: Philadelphia, 2002.
(6) Warburg, O. On the origin of cancer cells. *Science* **1956**, *123*, 309–314.
(7) Ishihara, M.; Togo, H. An Efficient Preparation of 2-Imidazolines and Imidazoles from Aldehydes with Molecular Iodine and (Diacetoxyiodo)benzene. *Synlett* **2006**, *2*, 227–230.
(8) Williams, D. R.; Lowder, P. D.; Gu, Y.-G.; Brooks, D. A. Studies of Mild Dehydrogenations in Heterocyclic System. *Tetrahedron Lett.* **1997**, *38*, 331–334.
(9) Haneda, S.; Okui, A.; Ueba, C.; Hayashi, M. An efficient synthesis of 2-arylimidazoles by oxidation of 2-arylimidazolines using activated carbon–O_2 system and its application to palladium-catalyzed Mizoroki–Heck reaction. *Tetrahedron* **2007**, *63*, 2414–2417.
(10) Amemiya, Y.; Miller, D. D.; Hsu, F.-L. Dehydrogenation of imidazolines to imidazoles with Pd-Carbon. *Synth. Commun.* **1990**, *20*, 2483–2489.
(11) Jones, H.; Fordice, M. W.; Greenwald, R. B.; Hannah, J.; Jacobs, A.; Ruyle, W. V.; Walford, G. L.; Shen, T. Y. Synthesis and analgesic-antiinflammatory activity of some 4- and 5-substituted heteroarylsalicylic acids. *J. Med. Chem.* **1977**, *21*, 1100–1104.
(12) Nakamura, T.; Sato, M.; Kakinuma, H.; Miyata, N.; Taniguchi, K.; Bando, K.; Koda, A.; Kameo, K. Pyrazole and isoxazole derivatives as new, potent, and selective 20-hydroxy-5,8,11,14-eicosatetraenoic acid synthase inhibitors. *J. Med. Chem.* **2003**, *46*, 5416–5427.
(13) Mahboobi, S.; Sellmer, A.; Burgemeister, T.; Lyssenko, A.; Schollmeyer, D. Synthesis of Naturally Occurring Pyrazine and Imidazole Alkaloids from *Botryllus Leachi*. *Monatsh. Chem.* **2004**, 333–342.
(14) Lee, J. P.; Lee, S. S. Kinetics and Mechanism for Hydrolysis Reaction of *N*-Benzoyl-2-phenylimidazole. *Bull. Korean Chem. Soc.* **2002**, *23*, 151–153.
(15) Bellina, F.; Cauteruccio, S.; Monti, S.; Rossi, R. Novel imidazole-based combretastatin A-4 analogues: evaluation of their in vitro antitumor activity and molecular modeling study of their binding to the colchicine site of tubulin. *Bioorg. Med. Chem. Lett.* **2006**, *16*, 5757–5762.
(16) Wang, L.; Woods, K. W.; Li, Q.; Barr, K. J.; McCroskey, R. W.; Hannick, S. M.; Gherke, L.; Credo, R. B.; Hui, Y.-H.; Marsh, K.; Warner, R.; Lee, J. Y.; Zielinski-Mozng, N.; Frost, D.; Rosenberg, S. H.; Sham, H. L. Potent, Orally Active Heterocycle-Based Combretastatin A-4 Analogues: Synthesis, Structure–Activity Relationship, Pharmacokinetics, and In Vivo Antitumor Activity Evaluation. *J. Med. Chem.* **2002**, *45*, 1697–1711.
(17) Ross, D. T.; Scherf, U.; Eisen, M. B.; Perou, C. M.; Rees, C.; Spellman, P.; Iyer, V.; Jeffrey, S. S.; Van de Rijn, M.; Waltham, M.; Pergamenschikov, A.; Lee, J. C.; Lashkari, D.; Shalon, D.; Myers, T. G.; Weinstein, J. N.; Botstein, D.; Brown, P. O. Systematic variation in gene expression patterns in human cancer cell lines. *Nature Genet.* **2000**, *24*, 227–235.
(18) Sellappan, S.; Grijalva, R.; Zhou, X.; Yang, W.; Eli, M. B.; Mills, G. B.; Yu, D. Lineage infidelity of MDA-MB-435 cells: expression of melanocyte proteins in a breast cancer cell line. *Cancer Res.* **2004**, *64*, 3479–3485.
(19) Rae, J. M.; Creighton, C. J.; Meck, J. M.; Haddad, B. R.; Johnson, M. D. MDA-MB-435 cells are derived from M14 melanoma cells—a loss for breast cancer, but a boon for melanoma research. *Breast Cancer Res. Treat.* **2007**, *104*, 13–19.
(20) Dong, X.; Mattingly, C. A.; Tseng, M. T.; Cho, M. J.; Liu, Y.; Adams, V. R.; Mumper, R. J. Doxorubicin and paclitaxel-loaded lipid-based nanoparticles overcome multidrug resistance by inhibiting P-glycoprotein and depleting ATP. *Cancer Res.* **2009**, *69*, 3918–3926.
(21) Leonessa, F.; Green, D.; Licht, T.; Wright, A.; Wingate-Legette, K.; Lippman, J.; Gottesman, M. M.; Clarke, R. MDA435/LCC6 and MDA435/LCC6MDR1: ascites models of human breast cancer. *Br. J. Cancer* **1996**, *73*, 154–161.
(22) Zhang, S.; Morris, M. E. Effects of the flavonoids biochanin A, morin, phloretin, and silymarin on P-glycoprotein-mediated transport. *J. Pharmacol. Exp. Ther.* **2003**, *304*, 1258–1267.
(23) Vredenburg, M. R.; Ojima, I.; Veith, J.; Pera, P.; Kee, K.; Cabral, F.; Sharma, A.; Kanter, P.; Greco, W. R.; Bernacki, R. J. Effects of orally active taxanes on P-glycoprotein modulation and colon and breast carcinoma drug resistance. *J. Natl. Cancer Inst.* **2001**, *93*, 1234–1245.
(24) Povlsen, C. O.; Jacobsen, G. K. Chemotherapy of a human malignant melanoma transplanted in the nude mouse. *Cancer Res.* **1975**, *35*, 2790–2796.
(25) Li, C.-M.; Lu, Y.; Narayanan, R.; Miller, D. D.; Dalton, J. T. Drug metabolism and pharmacokinetics of 4-Substituted Methoxybenzoyl-Aryl-Thiazoles (SMART). *Drug Metab. Dispos.* **2010**, doi:10.1124/dmd.110.034348.
(26) Lowe, J.; Li, H.; Downing, K. H.; Nogales, E. Refined structure of alpha beta-tubulin at 3.5 A resolution. *J. Mol. Biol.* **2001**, *313*, 1045–1057.
(27) Gigant, B.; Wang, C.; Ravelli, R. B.; Roussi, F.; Steinmetz, M. O.; Curmi, P. A.; Sobel, A.; Knossow, M. Structural basis for the regulation of tubulin by vinblastine. *Nature* **2005**, *435*, 519–522.
(28) Ravelli, R. B.; Gigant, B.; Curmi, P. A.; Jourdain, I.; Lachkar, S.; Sobel, A.; Knossow, M. Insight into tubulin regulation from a complex with colchicine and a stathmin-like domain. *Nature* **2004**, *428*, 198–202.
(29) Tahir, S. K.; Kovar, P; Rosenberg, S. H.; Ng, S. C. Rapid colchicine competition-binding scintillation proximity assay using biotin-labeled tubulin. *Biotechniques* **2000**, *29*, 156–160.
(30) Dorleans, A.; Gigant, B.; Ravelli, R. B.; Mailliet, P.; Mikol, V.; Knossow, M. Variations in the colchicine-binding domain provide insight into the structural switch of tubulin. *Proc. Natl. Acad. Sci. U.S.A* **2009**, *106*, 13775–13779.
(31) Rustin, G. J.; Shreeves, G.; Nathan, P. D.; Gaya, A.; Ganesan, T. S.; Wang, D.; Boxall, J.; Poupard, L.; Chaplin, D. J.; Stratford, M. R.; Balkissoon, J.; Zweifel, M. A Phase Ib trial of CA4P (combretastatin A-4 phosphate), carboplatin, and paclitaxel in patients with advanced cancer. *Br. J. Cancer* **2010**, *102*, 1355–1360.
(32) Glomme, A.; Marz, J.; Dressman, J. B. Comparison of a miniaturized shake-flask solubility method with automated potentiometric acid/base titrations and calculated solubilities. *J. Pharm. Sci.* **2005**, *94*, 1–16.
(33) Guo, W.; Wu, S.; Liu, J.; Fang, B. Identification of a small molecule with synthetic lethality for K-ras and protein kinase C iota. *Cancer Res.* **2008**, *68*, 7403–7408.